Single cell transcriptomics identifies adipose tissue CD271^{+} progenitors for enhanced angiogenesis in limb ischemia

Oto Inoue,[1,5] Chiaki Goten,[1] Daiki Hashimuko,[1] Kosei Yamaguchi,[1] Yusuke Takeda,[1] Ayano Nomura,[1] Hiroshi Ootsuji,[1] Shinichiro Takashima,[1] Kenji Iino,[2] Hirofumi Takemura,[2] Manasi Halurkar,[5] Hee-Woong Lim,[3,4] Vivian Hwa,[4,5] Joan Sanchez-Gurmaches,[4,5,6,*] Soichiro Usui,[1,*] Masayuki Takamura[1,7,*]

Affiliations:

[1]Department of Cardiovascular Medicine, Graduate School of Medical Sciences, Kanazawa University, Kanazawa, Japan

[2]Department of Thoracic, Cardiovascular and General Surgery, Graduate School of Medical Sciences, Kanazawa University, Kanazawa, Japan

[3]Division of Biomedical Informatics, Cincinnati Children's Hospital Medical Center, Cincinnati, Ohio, USA

[4]Department of Pediatrics, University of Cincinnati College of Medicine, Cincinnati, Ohio, USA

[5]Division of Endocrinology, Cincinnati Children's Hospital Medical Center, Cincinnati, Ohio, USA

[6]Division of Developmental Biology, Cincinnati Children's Hospital Medical Center, Cincinnati, Ohio, USA

[7]Lead contact

[*]**Correspondences: juan.sanchezgurmaches@cchmc.org (J.S.G.), usuiso@staff.kanazawa-u.ac.jp (S.U.), mtakamura@staff.kanazawa-u.ac.jp (M.T.)**

HIGHLIGHTS

- Adipose tissue stromal cells have a distinct angiogenic gene profile among human cell sources.
- CD271^{+} progenitors in adipose tissue have a prominent angiogenic gene profile.
- CD271^{+} progenitors show superior therapeutic capacities for limb ischemia.
- CD271^{+} progenitors are reduced and functionally impaired in insulin resistant donors.

GRAPHICAL ABSTRACT

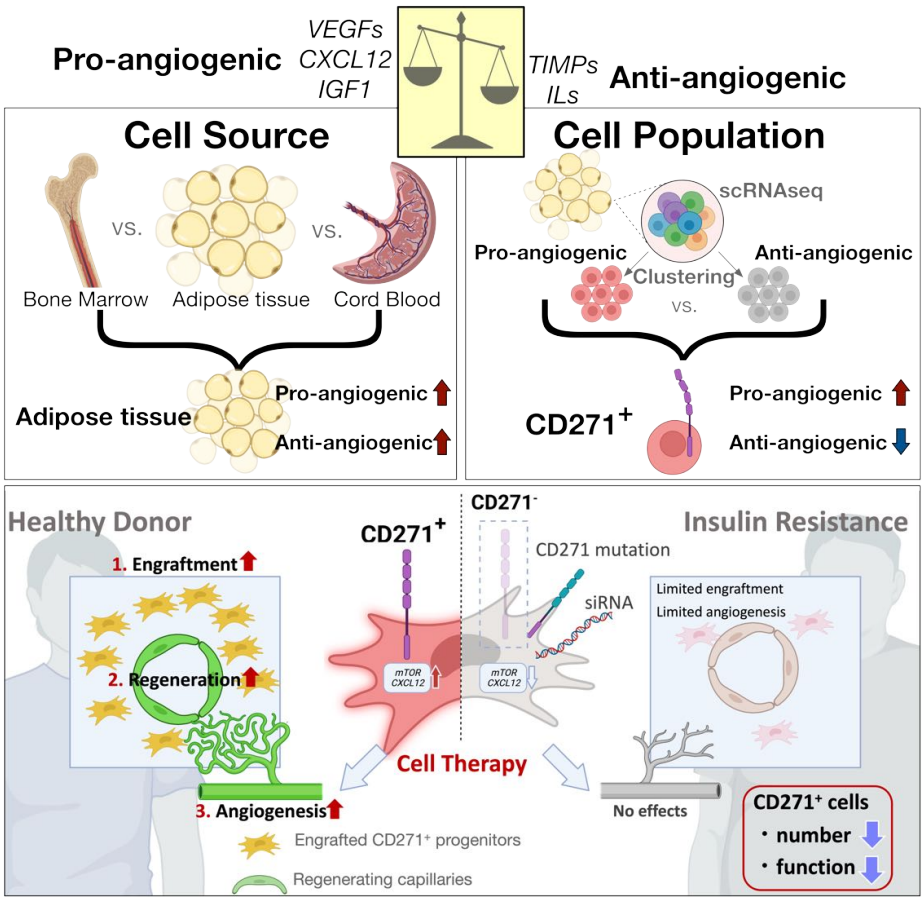

SUMMARY:

Therapeutic angiogenesis using mesenchymal stem/stromal cell grafts have shown modest and controversial effects in preventing amputation for patients with critical limb ischemia. Through single-cell transcriptomic analysis of human tissues, we identified CD271^{+} progenitors specifically from subcutaneous adipose tissue (AT) as having the most prominent pro-angiogenic gene profile distinct from other stem cell populations. AT-CD271^{+} progenitors demonstrated robust *in vivo* angiogenic capacity, over conventional adipose stromal cell grafts, characterized by long-term engraftment, augmented tissue regeneration, and significant recovery of blood flow in a xenograft model of limb ischemia. Mechanistically, the angiogenic capacity of CD271^{+} progenitors is dependent on functional CD271 and mTOR signaling. Notably, the number and angiogenic capacity of CD271^{+} progenitors was strikingly reduced in insulin resistant donors. Our study highlights the identification of AT- CD271^{+} progenitors with *in vivo* superior efficacy for limb ischemia. Furthermore, we showcase comprehensive single-cell transcriptomics strategies for identification of suitable grafts for cell therapy.

Keywords: single cell transcriptomics, therapeutic angiogenesis, cell therapy, CD271, adipose tissue, insulin resistance, peripheral artery disease, critical limb ischemia

47 **INTRODUCTION**

48 Critical limb ischemia (CLI), the end-stage of peripheral artery disease, is increasingly prevalent,
49 in part due to the worldwide increase in obesity and diabetes.[1] Prognosis for patients with CLI is
50 poor, comparable to malignant diseases.[2] One of the fatal features of CLI is atherosclerotic
51 calcification, a condition difficult to treat even with currently available revascularization
52 techniques such as catheter interventions and bypass surgery.[1] Consequently, at least 1 in 3 CLI
53 patients are not eligible for revascularization therapies.[3] To combat this, the strategy of inducing
54 neovascularization in ischemic tissues, known as therapeutic angiogenesis, has emerged as an
55 attractive alternative therapy for CLI.[4]

56 Mesenchymal stem/stromal cells with regenerative capacities were discovered from
57 multiple human organs including "harvestable" tissues such as bone marrow (BM), subcutaneous
58 adipose tissue (AT), and umbilical cord blood (UCB).[5] The main reported therapeutic mechanism
59 associated with cell therapy-induced neovascularization is through secretion of growth factors
60 (i.e., VEGF, HGF, SDF-1) and extracellular vesicles from injected cells. [6,7] Preclinical studies of
61 cell-based therapeutic angiogenesis using these cell sources showed favorable effects in animal
62 models,[7-11] but have translated poorly in clinical trials. [4,7] For CLI, unsorted BM mononuclear
63 cells are the most intensively evaluated in clinical trials. In a meta-analysis including 19
64 randomized controlled trials, cell therapy showed favorable effects on surrogate endpoints such

65 as pain score, pain-free walking distance, and ankle brachial index, but showed no significant
66 benefits on primary endpoints including amputation-free rate and complete ulcer healing[12].
67 Prospective isolation of specific cell populations from BM mononuclear cells, based on CD133^{+}
68 or CD34^{+} cells which were reported to be angiogenic preclinically,[10,13] also showed no evidence
69 for lowering the risk of limb amputation in clinical trials.[14-16] Thus, a suitable cell population(s)
70 optimal for therapeutic angiogenesis to achieve limb salvation has yet to be identified.
71 Single-cell transcriptomic technologies has revolutionized the capacity to identify
72 lineages in tissue homeostasis and markers of specific stem cell populations.[17-21] However,
73 application of single-cell transcriptomic analysis in cell therapy has been limited to only chimera
74 antigen receptor T (CAR-T) cell therapy for lymphoma, where important cell populations for
75 treatment response were assessed by single-cell RNA-sequencing (scRNA-seq). [22,23]
76 In this study, we took advantages of available scRNA-seq datasets generated from
77 different human tissues to screen for cell surface markers that allow the segregation of a highly
78 angiogenic subpopulation of cells. We identified that the CD271^{+} cells specifically from AT
79 have a distinct angiogenic gene profile with promising *in vivo* angiogenic capacity.
80 Mechanistically, CD271/mTOR axis showed an important role for *in vivo* angiogenic capacity.
81 Furthermore, we extend our findings to evaluate the feasibility and revascularization efficacy of
82 CD271^{+} cells from donors with cardiovascular disease (CVD). We obtained a sufficient number

83 of CD271^{+} progenitors from metabolically healthy CVD donors, and discovered superior

84 therapeutic potentials over conventional cell grafts for patients suffering from CLI.

RESULTS

Adipose Tissue Lineage-negative Cells Show a Distinct Angiogenic Gene Profile among Human Stem Cell Sources

There is a strong need to identify the most suitable cell source for therapeutic angiogenesis. To search for subpopulations with pro-angiogenic capacity, we explored single cell gene expression profiles from readily available human stem cell sources. We analyzed available scRNA-seq datasets from bone marrow (BM),[24] umbilical cord-blood (UCB),[25] and stromal vascular fraction (SVF) of subcutaneous adipose tissue (AT)[26] from healthy donors (***n*** = 2/tissue, **Figure 1A** and **Table S1**). We performed dimension reduction with t-distributed stochastic neighbor embedding (tSNE) and cell clustering of a total of 47,035 cells (**Figure 1A-B and Figure S1**). To annotate clusters, marker genes for each cluster were collated manually based on reported markers in the Human Cell Atlas and the Human Protein Atlas (proteinatlas.org, **Figure S1**). [19,27,28] We removed mature immune and endothelial cells, i.e. Lineage-positive (Lin^+) cells,[27] from further analysis to enrich stem/progenitor cell populations. Since classic lineage markers of immune and endothelial cells differ between tissues, and $CD31^+$ cells are reported to be angiogenic only in BM[11], we used a well-established but distinct set of lineage-markers in each of these tissues[29-31] (listed in **Figure 1A**). Overall, we processed 18,053 Lin^- cells (BM; 9,289, UCB; 1,932, and AT; 6,832 cells, **Figure 1B**).

103 The main mechanism of cell-based therapeutic angiogenesis has been reported to be
104 paracrine activities of soluble growth factors released by injected cells [6,32]. Thus, to further
105 characterize angiogenic gene profiles of stem cell sources, we used a gene set of reported
106 pro/anti-angiogenic factors released from tissue stem cells[6]. We updated the list with an
107 additional gene set of 38 well-known secreted pro-/anti-angiogenic factors [33-35] (**Table S2**).
108 Hierarchical clustering of BM, UCB, and AT Lin^- cells based on expression of pro-/anti-
109 angiogenic factor genes clearly isolates AT cells as having a distinctive gene expression profile.
110 This was characterized by prominent expression of pro-angiogenic factors including *MMP2*,
111 *CXCL12*, *VEGFs* and *IGF1* (**Figure 1C**). Consistently, gene enrichment analysis resulted in a
112 number of pro-angiogenic pathways which were significantly enriched in AT compared to BM or
113 UCB (**Figure 1D**). On the other hand, we observed that anti-angiogenic factors such as *TIMP2*
114 and *TIMP3* were also upregulated in AT (**Figure 1C**). Therefore, we hypothesized that AT would
115 be an attractive cell source if pro-angiogenic cells could be segregated from TIMP2/3 expressing
116 anti-angiogenic cells.

117 ***Adipose Tissue scRNA-seq Analysis Filtered 30 Surface Markers of Angiogenic Cells***

118 To delineate angiogenic populations within the AT, we analyzed Lin^-CD34^+ progenitors on
119 available scRNA-seq datasets from six non-diabetic human subcutaneous AT SVF (**Figure 2A**).
120 Louvain clustering divided AT Lin^-CD34^+ progenitor cells[8,36] into 3 progenitor groups (**Figure**

121 **2B and Figure S2A**). To understand the nature of each of these clusters, we analyzed the top 10
122 marker genes of each Progenitor cluster (**Figure 2C**). Progenitor 1 cluster was characterized by
123 higher expression of adipocyte lineage markers (*APOE,* and *CEBPD*), while Progenitor 2 by
124 mesenchymal/fibrotic markers (*FBN1*, *MFAP5*, and *FN1*). Progenitor 3 highly expressed some
125 adipocyte lineage markers common to Progenitor 1, including *APOD*, but was characterized by
126 higher expression of non-adipocyte markers *MYOC* and *IGFBP3*. Among these 3 clusters,
127 pathway enrichment analysis found that Progenitors 1 & 3 were dominated by genes involved in
128 sprouting angiogenesis and lipogenesis (**Figure 2D**). Based on this analysis, Progenitors 1 & 3
129 were defined as pro-angiogenic clusters while Progenitor 2 was defined as an anti-angiogenic
130 cluster. Using the same gene set as for cell source screening (**Figure 1C** and **Table S1**), we
131 compared pro/anti-angiogenic factor genes between the pro- and anti-angiogenic clusters. The
132 expression level of pro/anti-angiogenic factors clearly separates pro- and anti-angiogenic clusters
133 on our reanalyzed scRNA-seq datasets from six non-diabetic human subcutaneous AT SVF
134 (**Figure 2A, S2B**). Among the 38 genes in the gene set, 22 genes were differentially expressed
135 between pro/anti-angiogenic clusters. As expected, the pro-angiogenic cluster showed higher
136 expression of 12 pro-angiogenic factors, while all 5 anti-angiogenic factor genes were highly
137 expressed in the anti-angiogenic cluster (**Figure S2B**).
138 To obtain intact cell populations for cell therapy purposes, purification procedures

139 utilizing surface markers are necessary. Thus, we next focused on identifying the surface markers
140 specifically expressed in the pro-angiogenic cluster that would be suitable for downstream flow
141 cytometric isolation. Based on 2,621 differentially expressed genes between pro-/anti-angiogenic
142 clusters from scRNA-seq analysis identified when grouping data from the six samples analyzed
143 (**Figure 2E**, **Figure S2C and Table S3**), a total of 30 surface protein-encoding genes (**Table S4**)
144 were identified. We concluded that these 30 surface proteins may potentially lead to the specific
145 isolation of pro-angiogenic cells.

146 Next, we determined which marker from the filtered 30 surface protein-encoding genes
147 would be the most suitable for cell graft preparation for therapeutic angiogenesis. To achieve
148 this, we evaluated the specificity of the 30 individual surface proteins enriched in the pro-
149 angiogenic cluster by analyzing the number of cells that express each protein in each cluster
150 using the data from the same six non-diabetic human subcutaneous AT SVF (**Figure 2A, 2F**).
151 From this analysis, 5 surface markers were identified for isolating pro-angiogenic cells with over
152 95% purity (**Figure 2G**). Among them, CD271 (Low-affinitive nerve growth factor receptor,
153 LNGFR) emerged as the top-ranked surface marker, closely followed by VCAM1 (vascular cell
154 adhesion molecule 1) and ABCB11 (ATP binding cassette subfamily B member 11). In particular,
155 from the cells detected to express CD271, 98% were on the pro-angiogenic cluster (**Figure 2G**).
156 This is appreciably higher compared to $Lin^{-}CD34^{+}$ progenitors (Prog 1,2, and 3) and to other

157 previously known AT progenitor markers[37] such as CD105, CD90, and CD73 (**Figure 2G**).

158 Furthermore, out of the cells labelled by CD271 expression less than 3% were on the anti-

159 angiogenic cluster, which was the lowest contamination rate amongst all studied markers (**Figure**

160 **2G**). Thus, we identified surface markers that may efficiently select for pro-angiogenic cells.

161 ***Adipose Tissue CD271$^+$ Cells are Highly Angiogenic***

162 Next, we further analyzed the top three surface markers identified in our analysis aiming to find

163 which cell population showed the highest angiogenic potential. We noted that CD271$^+$,

164 VCAM1$^+$, and ABCB11$^+$ cell subpopulations are distinct, with very few cells carrying all three

165 markers, or even 2 of the 3 markers (**Figure 3A**). In particular, over 80% of CD271$^+$ cells were

166 VCAM$^-$/ABCB11$^-$. Therefore, we performed pathway enrichment analysis for subpopulations

167 carrying each single marker, i.e. comparing between CD271$^+$VCAM$^-$ABCB11$^-$, CD271$^-$

168 VCAM$^+$ABCB11$^-$, and CD271$^-$VCAM$^-$ABCB11$^+$. Strikingly, CD271$^+$ cells showed pro-

169 angiogenic pathway enrichment over VCAM1$^+$ or ABCB11$^+$ cell populations (**Figure 3B**).

170 Direct comparison between CD271$^+$ and CD271$^-$ populations showed that CD271$^+$ cells have

171 higher expression of important pro-angiogenic factors (e.g., *MCP1*, *CXCL12*, *CTGF*, and

172 VEGFA **Figure 3C**). Additionally, anti-angiogenic factors *TIMP2* and *TIMP3* were

173 downregulated in CD271$^+$ cells compared to CD271$^-$ cells (**Figure 3C**).

174 We next asked if it is possible to obtain sufficient number of CD271$^+$ cells from AT for

175 therapeutic angiogenesis. We found that the number of CD271 expressing cells were at least 10
176 times higher in AT than in BM or UCB (**Figure 3D**). To confirm these results, we performed
177 flow analysis on SVF cells of human subcutaneous AT. Consistently, we detected CD271 protein
178 in at least 5–10% of total SVF cells of human subcutaneous AT (**Figure 3G**); in contrast, it was
179 previously reported that less than 0.1% of individual BM cells expressed CD271 protein by flow
180 analysis.[38] From these data, we concluded that AT is the most suitable tissue for harvesting
181 sufficient number of $CD271^+$ cells.

182 Although AT carried higher numbers of $CD271^+$ cells than either BM or UCB, we
183 assessed whether $CD271^+$ cells are pro-angiogenic, independent of tissue source. As expected,
184 AT-$CD271^+$ cells showed strong enrichment in proangiogenic pathways when compared to AT-
185 $CD271^-$ cells (**Figure 3E**). BM-$CD271^+$ cells, in contrast, were characterized by pathways
186 related to the cell cycle and proliferation (**Figure 3E**), consistent with a previous report that BM-
187 $CD271^+$ cells possess clonogenic and multi-lineage differentiation capacities.[38] On the other
188 hand, UCB-$CD271^+$ cells showed upregulation of immune system-related pathways when
189 compared to UBC-$CD271^-$ (**Figure 3E**). These transcriptomic analyses indicated that although
190 $CD271^+$ cells are available from different tissues, AT-$CD271^+$ cells exhibit a distinct, pro-
191 angiogenic, gene profile.

192 It is of note that several subpopulations of BM, including $CD34^+$ [14], $CD133^+$ [16], and

193 CD31^{+} [11] populations, have been reported to be angiogenic and also have been tested in clinical

194 trials. Thus, we compared transcriptomic profile of AT-CD271^{+} cells to these three BM

195 subpopulations (**Figure 3F**). We found that AT-CD271^{+} cells consistently showed enrichment of

196 pathways related to cell differentiation while BM subpopulations were characterized by

197 involvement with immune systems. More importantly, AT-CD271^{+} cells demonstrated

198 enrichment of pro-angiogenic pathways (e.g. activating endothelial proliferation and VEGF

199 signaling) when compared to each BM subpopulation. Altogether, these transcriptomic data

200 indicate that AT-CD271^{+} cells has higher angiogenic potential than candidates already in clinical

201 trials.

202 ***AT-CD271^{+} progenitors are culture-expandable with classical mesenchymal stem cell capacity***

203 It is known that culture-expandable mesenchymal stem cell-like cells can be generated

204 from unsorted AT-progenitors, and are commonly referred as adipose-derived stem cells

205 (ADSCs) [39]. To better understand human AT-CD271^{+} cell biology, we sorted and established *in*

206 *vitro* cultures of CD271^{+} and CD271^{-} cells from subcutaneous AT of human healthy subjects

207 (**Figure 3G**). Both types of cells were adherent and proliferative with similar spindle-shaped

208 morphology (**Figure 3H**). CD271^{+} cells, however, showed enhanced proliferative capacity

209 compared to CD271^{-} cells as determined by colony formation assay where CD271^{+} cells

210 generated larger and more dense colonies (**Figure 3H**) in significantly higher number (**Figure**

211 **3I**). Both cell types readily differentiated into adipocyte (Oil Red O) and osteoblast (Alizarin

212 Red) lineages (**Figure 3J**). Collectively, these *in vitro* assays characterized CD271$^+$ progenitors

213 as culture-expandable with classical ADSC morphology and capacities.[39]

214 ***CD271$^+$Progenitors Demonstrate Enhanced In Vivo Angiogenic Capacity with Long-Term***

215 ***Engraftment***

216 We next examined the *in vivo* angiogenic capacity of CD271$^+$ progenitors in a xenograft model

217 of limb ischemia (**Figure 4A**). For this, we injected PKH-labeled human CD271$^+$ or CD271$^-$

218 progenitors (0.5 million cells / mice) directly into limb muscles of immunocompromised mice

219 that are subjected to left femoral artery ligation. Cell-treated limbs were harvested at day 7, 14,

220 and 35 after fluorescence-conjugated isolectin perfusion to detect capillaries with blood flow

221 [9,30,40].

222 In this xenograft model, we observed that CD271$^+$ progenitors clearly engrafted better

223 than CD271$^-$ progenitors in ischemic limb, with 2-3 times higher PKH$^+$ cell numbers (**Figure**

224 **4B-C**). The enhanced differences in engraftment capacity of AT-CD271$^+$ progenitors persisted

225 for up to 5 weeks. Further, immunofluorescent analysis of tissue sections shows that AT-CD271$^+$

226 progenitors localize around lectin$^+$ capillaries (**Figure S3A**). To clarify whether injected CD271$^+$

227 progenitors were potentially trans-differentiating to endothelial cells, we performed flow

228 cytometric analysis of PKH$^+$ cells from digested limb muscles 14 days after cell engraftment

229 (**Figure S3B**). We confirmed that only 6% of engrafted CD271$^+$ progenitors expressed the
230 endothelial marker CD31, which suggested the majority of the injected cells did not undergo
231 differentiation into mature endothelial cells, at least not within the time frame of the protocol
232 (**Figure S3C**). On the other hand, isolated PKH$^+$ cells maintained expression of human CD271
233 and typical markers of cultured ADSCs[37] (human CD90 and CD105) (**Figure S3C**). These
234 findings confirmed that engrafted CD271$^+$ progenitors preserve their stem cell marker
235 expressions and likely acted as stem/progenitor cells to support intrinsic regeneration.

236 Correlating with higher survival of engraftment, CD271$^+$ progenitor therapy induced
237 enhanced revascularization after limb ischemia. This is evidenced by 3-fold higher capillary
238 density (Lectin$^+$ and mouse CD31$^+$, **Figure S3D**) than that induced by CD271$^-$ progenitors
239 (**Figure 4D**). Strikingly, CD271$^+$ progenitors successfully led to recovery of blood flow in
240 treated limb, to a level comparable to healthy limbs, as determined by both imaging and doppler
241 blood flow analysis (**Figure 4E-F**).

242 To confirm tissue reparative capacity of CD271$^+$ progenitors, we incorporated *in vivo*
243 EdU labeling into our *in vivo* protocol (**Figure 4G**). Since neovascularization and blood flow
244 recovery were favorably accomplished by day 14 in our model, we evaluated EdU incorporation
245 on day 7 when tissue neovascularization was in progress. *In vivo* EdU labeling demonstrated that
246 treatment with CD271$^+$ progenitors led to approximately four times higher proliferation of host

247 cells (largely composed of skeletal muscle cells and endothelial cells and identified as PKH$^-$)

248 than treatment with CD271$^-$ progenitors (**Figure 4H-I**). Collectively, the data from our xenograft

249 model provide promising translational *in vivo* angiogenic capacity of CD271$^+$ progenitors with

250 long-term engraftment and enhanced host cell proliferation.

251 ***Mutant CD271 Impairs the Angiogenic Gene Profile and Therapeutic Capacity of mouse***

252 ***ADSCs***

253 We next explored potential mechanisms that drove angiogenic capacity of CD271$^+$ progenitors.

254 Reanalysis of scRNA-seq datasets of SVF cells from neonatal mice inguinal fat pads[41]

255 subclustered cells into 10 clusters (**Figure 5A and Figure S4A-B**). CD271$^+$ progenitors were

256 distributed predominantly with Schwann cell, pericytes, and Lin$^-$ Progenitor clusters (**Figure**

257 **S4B**). Consistent with human CD271$^+$ progenitors gene expression profiles (**Figure 3C**), mouse

258 CD271$^+$ showed upregulation of pro-angiogenic factors including *Igf1* and *Cxcl12*, and

259 downregulation of anti-angiogenic factors *Timp2* and *Timp3*. (**Figure 5B**). Furthermore, mouse

260 AT-CD271$^+$ progenitors showed enrichment of angiogenesis-related GO terms (endothelial cell

261 proliferation and VEGF signaling pathway, **Figure 5C**). We asked whether a functional CD271

262 protein is necessary for the angiogenic capacity of CD271$^+$ progenitors in mice. We used mice

263 lacking exon 3 of the CD271 gene which encodes three of the four necessary cysteine-rich

264 repeats in the extracellular domain. The loss of exon 3 generated an in-frame mutant CD271

265 protein with a 2- to 3-fold reduction in ligand binding[42] (**Figure 5D**). We established cultured
266 mouse ADSCs from wild-type littermates (Control) and CD271 mutant mice ($CD271^{Mut}$).
267 Compared to Control-ADSCs, $CD271^{Mut}$ ADSC transplants demonstrated impaired cell
268 engraftment (**Figure 5E-F**), impaired *in vivo* angiogenesis (**Figure 5G**), and reduced blood flow
269 recovery (**Figure 5H-I)**. This data suggests that normal CD271 activity is required for $CD271^{+}$
270 cells to have full angiogenic capacity. This highlights an important new biological function of
271 CD271 and proposes the concept that CD271 is not only a surface marker for cell selection.
272 We asked what downstream signaling pathways of CD271 may participate in the
273 angiogenic functions of $CD271^{+}$ progenitors. CD271 can induce cell death or cell survival,
274 depending on interacting coreceptors.[43] Among the three known coreceptors of CD271,
275 tropomyosin receptor kinase B (TRKB), which coordinates with the mTOR pathway for cell
276 survival[44] (**Figure S5A**), was predominantly expressed in human AT-$CD271^{+}$ progenitors while
277 cell expressing the other coreceptors were rarely found (**Figure S5B**). We confirmed that over
278 95% of $CD271^{+}$ progenitors co-expressed TRKB protein even under cultured condition (**Figure**
279 **S5C**). Cultured $CD271^{+}$ progenitors also showed higher expression of *MTOR* than $CD271^{-}$
280 progenitors (**Figure S5D**). Furthermore, the known downstream genes regulated by mTOR
281 signaling, i.e., *HIF1A* and *VEGFA*, were significantly upregulated in $CD271^{+}$ progenitors
282 compared to $CD271^{-}$ (**Figure S5D**). Consistent with previous reports of positive feedback

283 between mTOR and SDF-1 (CXCL12)[45], *CXCL12* was also highly expressed in CD271^{+}

284 progenitors (**Figure S5D**). Interestingly, we noted that in mouse CD271^{Mut} ADSCs, *Mtor*

285 expression was reduced by ~50% (**Figure S5E**), which resulted in concomitant inhibition of

286 downstream factors *Hif1a*, *Vegfa*, and *Cxcl12* (**Figure S5E**). From these observations, we

287 hypothesized that the downstream mTOR pathway activated by CD271 may be required for the

288 angiogenic capacity of CD271^{+} progenitors. To test this hypothesis, we knockdown mTOR in

289 human ADSCs (cultured unsorted AT cells) using short interfering RNAs (si-mTOR ADSCs).

290 Gene expression analysis showed efficient knockdown of mTOR (**Figure S5F**). Additionally, si-

291 mTOR ADSCs shown downregulated expression of *VEGFA* and *CXCL12* (**Figure S5F**). Next,

292 we functionally tested the effects of decreased mTOR levels in cell therapy experiments using

293 our ischemic limb mouse model. si-mTOR treatment resulted in loss of *in vivo* angiogenic

294 capacity of ADSCs as evaluated by capillary density (**Figure S5G-H**), engraftment (**Figure S5I**)

295 and tissue reparative capacity evaluated by the number of proliferating cells (**Figure S5J-K**).

296 Together, our findings strongly suggest that a functional CD271/mTOR axis is necessary for full

297 ADSC angiogenic capacities.

298 ***CD271^{+} Progenitors from Insulin Resistant Patients are Decreased and Have Poor***

299 ***Therapeutic Potential***

300 Next, we asked if AT-CD271^{+} progenitors are available in sufficient number to be used in clinical

301 settings. For this, we analyzed patient-derived AT samples. First, we evaluated the number of
302 $CD271^+$ progenitors in subcutaneous AT from 38 CVD patients with various pathological
303 conditions and diseases (**Table S4).** The frequency of $CD271^+$ progenitors in SVF cells
304 ($CD271^+$/SVF) ranged from 0.2 to 40% and was not significantly affected by donor sex, BMI, or
305 age (**Figure 6A**). This is clearly favorable for cell preparation from a variety of donors.
306 Intriguingly, the number of $CD271^+$ progenitors was negatively correlated with the insulin
307 resistance score (HOMA-IR) (**Figure 6A**). Consistently, $CD271^+$ progenitor number was reduced
308 by approximately 75% in patients with insulin resistance (HOMA-IR > 2.9)[46] as determined by
309 flow cytometry (**Figure 6B**). Because immune cells accumulate in insulin-resistant AT, we
310 additionally calculated the percentage of $CD271^+$ progenitors in Lin^-CD34^+ cells. Consistently,
311 $CD271^+$/Lin^-CD34^+ SVF was also significantly reduced in patients with insulin resistance
312 (**Figure 6B**). To validate the finding of our 38 CVD patient cohort with an orthogonal method,
313 we analyzed available subcutaneous AT scRNA-seq datasets from lean healthy (insulin sensitive)
314 subjects versus obese type 2 diabetic (insulin resistant) subjects (**Figure 6C and Figure S6A**).
315 We found a significant reduction in the number of $CD271^-$ expressing cells in AT from insulin
316 resistant subjects (**Figure 6D-E**). Furthermore, GO enrichment analysis shows decreased
317 angiogenesis-related terms in $CD271^+$ progenitors from insulin resistant donors when compared
318 to $CD271^+$ progenitors from insulin sensitive donors (**Figure 6F and Table S5**).

319 Since our results show that CD271$^+$ progenitors have a positive therapeutic effect in our
320 mouse ischemic limb model, we next hypothesized that CD271$^+$ progenitor therapy is more
321 beneficial over conventional unsorted ADSCs in our model. Hence, we prepared paired unsorted
322 ADSCs and sorted CD271$^+$ progenitors from 5 insulin resistant and 5 insulin sensitive patient
323 subgroups from our 38-patient cohort (**Figure 6A-B**) to test their therapeutic effectiveness in our
324 ischemic limb mice model (**Figure 6G**). As shown in **Figure 6H**, sorted human CD271$^+$
325 progenitors showed markedly enhanced engraftment over conventional ADSCs from the same
326 donors. Notably, cell therapy with CD271$^+$ progenitors of metabolically healthy donors resulted
327 in improved engraftment than CD271$^+$ progenitors of insulin resistant donors (**Figure 6H**).
328 Interestingly, although CD271$^+$ progenitors from both insulin resistant and metabolically healthy
329 donors increased capillary density compared to respective unsorted cells, CD271$^+$ progenitors of
330 metabolically healthy donors achieved striking higher capillary density than those from insulin
331 resistant donors (**Figure 6I**). It is important to note that conventional unsorted ADSCs from
332 insulin resistant donors showed capillary density equivalent to PBS injection suggesting very
333 limited effect of this population (**Figure 6I**). Finally, CD271$^+$ progenitors from insulin sensitive
334 donors achieved full recovery of blood flow (**Figure 6J**) while CD271$^+$ progenitors from insulin
335 resistant donors were less effective but still achieved a remarkable > 85% recovery. These data
336 further highlight the promising efficacy of CD271$^+$ progenitor therapy for ischemic limb, even

337 from insulin resistant donors, albeit therapy from insulin sensitive donors may lead to better
338 long-term outcomes as engraftment is higher and improve the angiogenic capacity of the
339 ischemic lesion.

340 ***Preliminary Positive Impacts of Autologous CD271$^+$ Progenitors in a Trial Outcome of SVF***
341 ***Therapy for CLI***

342 To further investigate the therapeutic potential of CD271$^+$ progenitors, we retrospectively
343 evaluated data from a limited human cell therapy trial (multi-center clinical trial of SVF therapy)
344 for no-option CLI patients[47] (**Figure 7A** and **7B**). During the one-year follow-up period, patients
345 received no interventional treatments (e.g. catheter intervention, surgery). Medications were
346 already optimized prior to SVF therapy under consensus guidelines, and no further changes were
347 made [48]. Of the 4 patients within our trial who underwent SVF therapy (**Table S6**), 2 patients
348 exhibited complete recovery (disappearance of ulcer lesion, **Figure S7**) and 2 cases resulted in
349 either major amputation or ulcer recurrence at the 1-year follow-up post-SVF therapy (**Figure 7B**
350 and **7D**). All 4 patients had HOMA-IR within normal range (min-max 0.3-2.0, mean 1.4, **Table**
351 **S7**). Based on the above results, we hypothesized that successful recovery at the 1-year follow up
352 is correlated to the number of CD271$^+$ progenitors initially injected. Thus, we retrospectively
353 evaluated the potential impact of injected CD271$^+$ progenitor number on efficacy of SVF therapy
354 (**Figure 7C**). Then, we stratified patients based on recurrence or amputation outcome and

355 revisited the composition of cell initially injected. Although patient number in this analysis is
356 very small, we observed that our primary outcome does not correlate with total SVF nor with the
357 $Lin^{-}CD34^{+}$ cell number injected (**Figure 7E**). In particular, patient 2 who required amputation,
358 had received the highest dose of total SVF cells and $CD34^{+}$ cells compared to those of the
359 patients who recovered, suggesting that high doses of $CD34^{+}$ cells was insufficient for
360 preventing amputation. However, both patients that completely recovered from ulcers without
361 recurrence (patient 1 and 4) were injected with higher number of $CD271^{+}$ cells (**Figure 7E**). As
362 an example, Patient 1, who recovered from CLI, had approximately 200 times higher number of
363 $CD271^{+}$ progenitors injected than patient 3 who presented with recurrent ulceration (**Figure 7C**
364 and **F**). The positive correlation between full recovery and $CD271^{+}$ progenitors injected was
365 striking especially when we compared the number of injected $CD271^{+}$ progenitors per ulcer area
366 (***n*** = 6 ulcer lesions, **Figure 7F**). Collectively, our findings from this sub-analysis of SVF therapy
367 for CLI, strongly support the significance and positive therapeutic effects of $CD271^{+}$ progenitors.

368 **DISCUSSION**

369 Despite decades of research in therapeutic angiogenesis, the ideal cell population for grafting
370 remains to be fully determined. This is evidenced by controversial effects on amputation
371 prevention in 19 RCTs (837 patients) using 5 cell types[12]. In this study, we used unbiased single-
372 cell transcriptomics to identify adipose tissue CD271^{+} progenitors as a human pro-angiogenic
373 cell population with the strongest potential for efficacious therapeutics. Traditionally, the
374 identification of cell populations suitable for cell therapy had depended on biased selection of
375 markers, from which appropriate marker-positive cell populations were isolated for in-depth
376 analysis *in vitro* and *in vivo*. This potential hit-and-miss strategy is time consuming and costly,
377 and allow the analysis of only a limited number of markers.[49] In this study, we took advantage of
378 current single cell genomic approaches to simultaneously explore all known/detected surface
379 markers. Based to these unbiased analyses of available scRNA-seq datasets, we found that AT-
380 CD271^{+} progenitors were predominantly pro-angiogenic with less than 3% of antiangiogenic
381 cells. We suggest that application of single-cell transcriptomics for cell therapy can greatly
382 improve discovery of better cell markers for targeted therapies of interest. Furthermore, we took
383 advantage of evaluating cell populations with opposing functions through scRNAseq analysis,
384 i.e. therapeutic (pro-angiogenic) and harmful (anti-angiogenic) populations. Although an extra
385 purification step to exclude anti-angiogenic cells was not necessary due to the extremely low rate

386 of anti-angiogenic cells in CD271^{+} progenitors, sorting methodologies to isolate therapeutic
387 marker-positive away from harmful marker-negative cells could be strategic. For example,
388 immune-modulatory cell therapy for graft-versus-host disease,[50,51] which is increasingly
389 evaluated in clinical trials but with inconsistent outcomes, might benefit from such a strategy to
390 avoid pro-inflammatory cell engraftment.

391 The relationship between CD271 expression and cell angiogenic capacity has been
392 poorly established. There is a report demonstrating that CD271^{+} progenitors secreted angiogenic
393 factors *in vitro*.[52] However, limited angiogenesis was concomitantly observed in a mouse model
394 of CD271^{+} cell injection for cartilage repair.[53] Based on our present results, CD271^{+} progenitors
395 could exhibit angiogenic capacity specifically in ischemic-type diseases. Interestingly, previous
396 demonstrations that CD271^{+} cell/HUVEC coculture, but not conditioned medium, could enhance
397 the tube formation of HUVECs, suggest the importance of cell-to-cell interactions between
398 CD271^{+} progenitors and target cells. [52,53] In our xenograft model, we observed CD271^{+}
399 progenitors were surrounding capillaries and labeled by perfused lectin as with capillaries
400 (**Figure 4B-C** and **Figure S3A**). This indicates the close proximities between "leaky" capillaries
401 and engrafted cell grafts. Taken together, we conclude engraftment capability and cell-cell
402 interactions between cell grafts and the regenerating (immature) capillaries would be important
403 for CD271^{+} progenitors to exert angiogenic functions.

404 CD271, also known as LNGFR, is a transmembrane receptor originally found to be a
405 marker for neural lineage cells. CD271 is known to activate mTOR through cooperation with
406 coreceptors including TRKB, also known as NTRK2 (neurotrophic receptor tyrosine kinase 2)
407 [43,54] a coreceptor which we found to be abundantly expressed in the majority of CD271^{+}
408 progenitors from human SVF cells. Data from single-cell transcriptomics, mutant CD271 mouse
409 model, and mTOR silencing studies, all supported the participation of CD271/mTOR axis in the
410 angiogenic capacity of CD271^{+} progenitors. However, our si-mTOR studies may reflect general
411 blunted impacts since the mTOR pathway is a well-established major signaling hub for multiple
412 factors [55,56]. Our results, nevertheless, highlight the importance of mTOR activity for evaluating
413 ADSC quality. Future studies should assess whether neurotrophic factors may enhance
414 CD271/TRKB/mTOR signaling in CD271^{+} progenitors and if neurotrophin pretreatment or
415 controlled CD271 overexpression might be preconditioning strategies for enhancing angiogenic
416 effects of cell grafts.

417 In this study, we observed proliferative and angiogenic capacity of AT-CD271^{+}
418 progenitors. We found that angiogenic AT-CD271^{+} progenitor populations were reduced in
419 patients with insulin resistance, although the causal relationship between AT-CD271^{+} progenitor
420 decrease and insulin resistant is unclear from our study. Since blunted mTOR signaling in AT can
421 lead to insulin resistance,[44,57] the CD271/mTOR axis in AT may have protective roles against

422 insulin resistance. This may be important under obesogenic stimuli (e.g., overfeeding), when AT
423 dramatically increases its size and appropriate angiogenesis is essential in obesity to prevent
424 hypoxia which triggers AT inflammation and subsequently insulin resistance.[58-61] Future detailed
425 investigations of the CD271/mTOR axis in AT will provide better understanding of insulin
426 resistance pathophysiology and may reveal novel strategies to prevent metabolic syndrome.
427 Although preclinical studies suggested promising efficacy of cell therapy, clinical trials
428 have shown inconsistent results. This might be explained by numerical or functional differences
429 of cell grafts among CVD patients [62,63]. In this study, we demonstrated decreased cell number
430 and functional impairment of $CD271^+$ progenitors in insulin resistant donors. Given the higher
431 incidence of metabolic disorders in CVD patients, our findings have great implications for
432 effective cell therapy in CVD. It is critical to overcome the reduction in cell number and the
433 functional impairment of $CD271^+$ progenitors in insulin resistant donors if efficient $CD271^+$ cell
434 therapy is to be developed. We and others have previously reported altered gene expression and
435 impaired angiogenic effects of ADSCs derived from type 2 diabetic patients compared to ADSCs
436 from nondiabetics.[64,65] In this study, we found that HOMA-IR can be used as a surrogate marker
437 to predict quantity and quality of $CD271^+$ progenitors in AT. Therefore, HOMA-IR evaluations
438 may mitigate ineffective therapeutic interventions by permitting screening of appropriate donors
439 for therapeutic angiogenesis, not only for autologous therapy, but also for allograft (cell bank)

440 development.

441 Our single cell transcriptomics from multiple stem cell sources captured AT as a better
442 cell source for angiogenic cell populations than current BM mononuclear cells. Furthermore, we
443 showed $CD34^+$ selection did not increase the quantity of appropriate angiogenic cell population
444 when compared to unsorted SVF (**Figure 2H**). Here, we propose that targeted CD271 selection
445 is a novel strategy for preparing cell graft with $CD271^+$ progenitor therapy expected to improve
446 cell therapeutic outcomes. Although $CD271^+$ progenitors showed more angiogenic gene profiles
447 over the other candidate cell populations we screened (ABCB11 and VCAM1) or previously
448 reported (BM-$CD34^+$, $CD133^+$, and $CD31^+$), we did not compare angiogenic capacity directly in
449 this study. Further studies to compare $CD271^+$ progenitors and other potential subpopulations *in*
450 *vitro* and *in vivo* would be important to develop the most suitable strategy for therapeutic
451 angiogenesis. More importantly, as demonstrated in this study (**Figure 6** and **7**), the
452 feasibility/accessibility of these cell populations in human donors should be tested to
453 successfully translate our findings into clinical trials.

454 Our retrospective analysis of the SVF therapy trial for terminal CLI [47] supports a
455 positive correlation between complete recovery and high numbers of injected $CD271^+$
456 progenitors, while amputated/recurrence of CLI was associated with low numbers. Importantly,
457 we determined that approximately 300,000 to 500,000 AT-$CD271^+$ progenitors per lesion area

458 (CD271$^+$ cells / ulcer cm^2) as the dose that seems to be necessary for favorable outcome.

459 Fortunately, this is a dose which, in our experience, should be readily feasible to prepare from

460 CVD patients. Future studies and clinical trials focusing on CD271$^+$ progenitor therapy in larger

461 cohorts will provide the necessary clinical evidence for efficacy and dosing requirements.

462 In summary, we applied single-cell transcriptomics for cell therapy purposes against

463 CLI and identified a human stem cell population which is readily available and possesses the

464 most angiogenic gene profile. CD271$^+$ progenitors can be readily harvested from human

465 subcutaneous AT and exhibit promising angiogenic capacities, including long-term engraftment

466 and augmentation of host tissue cell proliferation in cell therapy. In CVD patients with systemic

467 insulin resistance, the number and angiogenic capacity of CD271$^+$ progenitors were significantly

468 decreased. CD271$^+$ progenitors obtained from insulin sensitive donors, in contrast, demonstrated

469 the highest *in vivo* angiogenic capacity and consistently rescued ischemic limb. Our data

470 highlight the potential screening benefits using single-cell technologies and evident benefits of

471 CD271$^+$ progenitor transplantation for improving current therapeutic angiogenesis.

472

473 **Study Limitations**

474 In this study, the correlation between the expression levels of CD271 mRNA and protein was not
475 directly analyzed. Although we confirmed higher mRNA expression of CD271 in sorted $CD271^+$
476 progenitors (data not shown), further studies using single-cell multiomics technologies, including
477 CITE-seq,[66] would be helpful to validate our results.

478 In mouse ADSC experiments, we observed that a mutation of the CD271-encoding gene
479 decreased angiogenic factor expression and impaired *in vivo* angiogenic capacity in unsorted
480 mouse ADSCs. We did not sort $CD271^+$ cells from $CD271^{Mut}$ mice because of difficulties in
481 detecting mutated CD271 with currently available monoclonal antibodies.

482 Finally, we could not definitely determine whether injected $CD271^+$ progenitors
483 transdifferentiate into endothelial cells or not. Although expression of human CD31 was
484 observed in only a small proportion of engrafted $CD271^+$ progenitors, the histological
485 assessment demonstrated that they were morphologically similar to stromal or perivascular cells
486 than to endothelial cells. Single-cell analysis of regenerating tissues after cell therapy might
487 provide more detailed information about the transcriptomic dynamics of injected $CD271^+$
488 progenitors.

489

ACKNOWLEDGEMENTS

We would like to acknowledge the support and collaborations of Professor Toyoaki Murohara, Dr. Rei Shibata, Dr. Yuuki Shimizu, and TACT-ADRC multicenter trial Group regarding SVF therapy trial. Additionally, we appreciate Professor Yoh Takuwa and Dr. Kazuaki Yoshioka for the assistance in Laser Doppler analysis for blood flow quantification. Furthermore, we thank Dr. Jun Kinoshita, Dr. Katsunobu Oyama, Dr. Yukio Fushida, and the other operating staff of Kanazawa University Hospital for providing adipose tissue samples to this study. Finally, we appreciate the study participants and their families. Diagrams in Figures were created with BioRender.com.

FUNDING

This study has been supported by Japan Society for the Promotion of Science (JSPS) KAKENHI (Tokyo, Japan) Grant Number JP16H06828. OI is supported by Japanese Heart Foundation Research Abroad Award 2021. JSG is supported by grants from the American Heart Association (18CDA34080527), the NIH (R21OD031907), a CCHMC Trustee Award, a CCHMC Center for Pediatric Genomics Award and a CCHMC Center for Mendelian Genomics & Therapeutics Award. The content is solely the responsibility of the authors and does not necessarily represent the official views of the National Institutes of Health.

AUTHOR CONTRIBUTIONS

Conceptualization: O.I., V.H., J.S.G., S.U., M.T.

Methodology: O.I., C.G., D.H., K.Y., Y.T., A.N., H.M., J.S.G., S.U.

Validation: O.I., C.G., D.H., K.Y., Y.T., A.N., H.M., J.S.G., S.U.

Formal Analysis: O.I., A.N., D.H., K.Y., H.W.L., J.S.G., S.U.

Investigation: O.I., C.G., D.H., K.Y., Y.T., A.N., H.O., S.T., H.M., H.W.L., J.S.G., S.U.

Resources: K.I., H.T.

Data Curation: O.I., H.W.L., V.H., J.S.G., S.U.

Writing – Original Draft: O.I., C.G., V.H., J.S.G., S.U., M.T.

Writing – Review & Editing: O.I., C.G., D.H., K.Y., Y.T., A.N., H.O., S.T., K.I., H.T., H.M., H.W.L., V.H., J.S.G., S.U., M.T.

Visualization: O.I., H.W.L., V.H., J.S.G., S.U.

Supervision: J.S.G., S.U., M.T.

Project Administration: J.S.G., S.U., M.T.

Funding Acquisition: J.S.G., S.U., M.T.

COMPETING INTERESTS

The authors declare no competing interests.

Figure 1

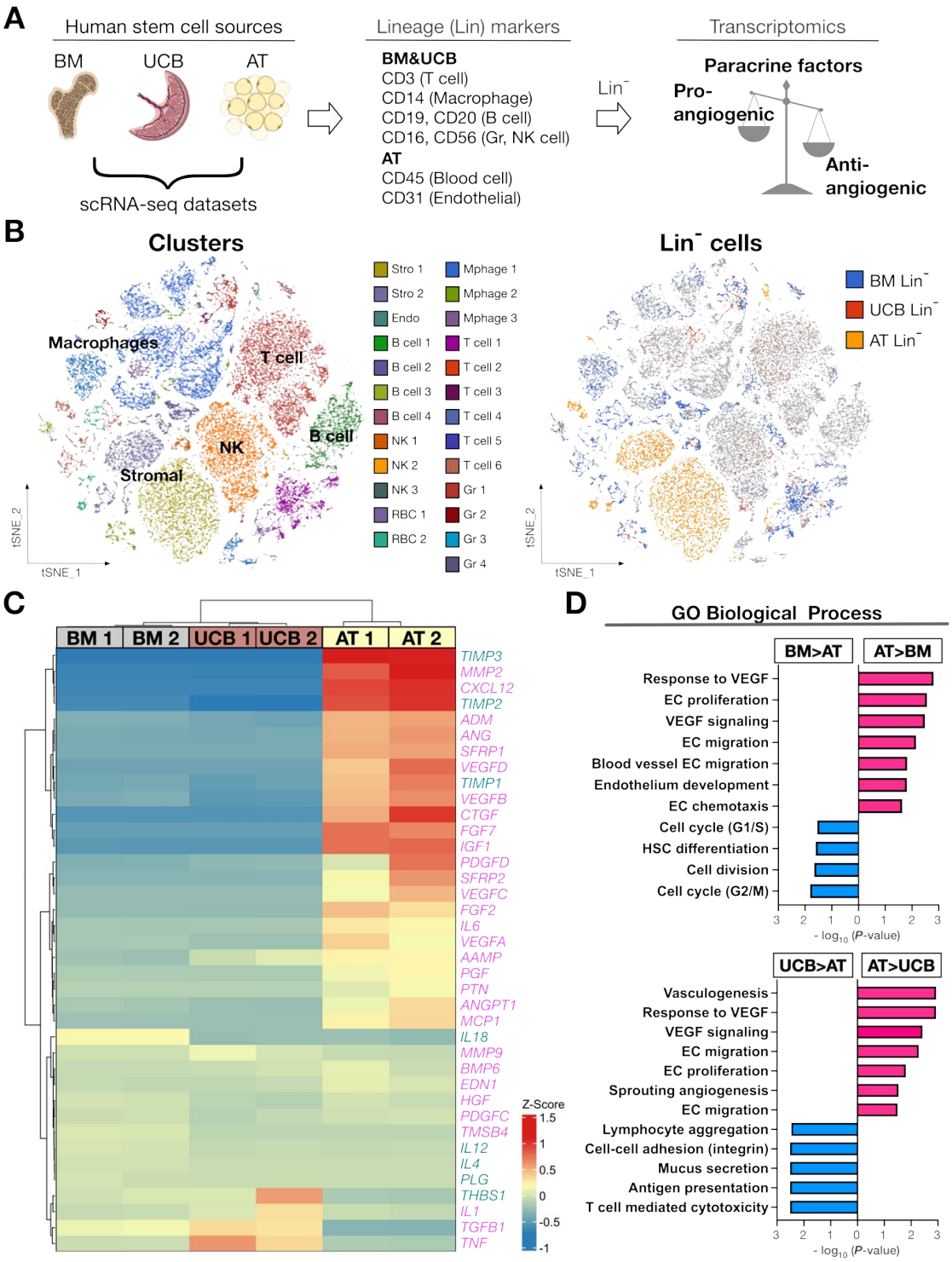
A
Human stem cell sources
BM
UCB
AT
scRNA-seq datasets
Lineage (Lin) markers
BM&UCB
CD3 (T cell)
CD14 (Macrophage)
CD19, CD20 (B cell)
CD16, CD56 (Gr, NK cell)
AT
CD45 (Blood cell)
CD31 (Endothelial)
Lin⁻
Transcriptomics
Paracrine factors
Pro-angiogenic
Anti-angiogenic
B
Clusters
Macrophages
T cell
B cell
NK
Stromal
tSNE_1
tSNE_2
Stro 1
Stro 2
Endo
B cell 1
B cell 2
B cell 3
B cell 4
NK 1
NK 2
NK 3
RBC 1
RBC 2
Mphage 1
Mphage 2
Mphage 3
T cell 1
T cell 2
T cell 3
T cell 4
T cell 5
T cell 6
Gr 1
Gr 2
Gr 3
Gr 4
Lin⁻ cells
BM Lin⁻
UCB Lin⁻
AT Lin⁻
C
BM 1
BM 2
UCB 1
UCB 2
AT 1
AT 2
TIMP3
MMP2
CXCL12
TIMP2
ADM
ANG
SFRP1
VEGFD
TIMP1
VEGFB
CTGF
FGF7
IGF1
PDGFD
SFRP2
VEGFC
FGF2
IL6
VEGFA
AAMP
PGF
PTN
ANGPT1
MCP1
IL18
MMP9
BMP6
EDN1
HGF
PDGFC
TMSB4
IL12
IL4
PLG
THBS1
IL1
TGFB1
TNF
Z-Score
1.5
1
0.5
0
-0.5
-1
D
GO Biological Process
BM>AT
AT>BM
Response to VEGF
EC proliferation
VEGF signaling
EC migration
Blood vessel EC migration
Endothelium development
EC chemotaxis
Cell cycle (G1/S)
HSC differentiation
Cell division
Cell cycle (G2/M)
- log10 (P-value)
UCB>AT
AT>UCB
Vasculogenesis
Response to VEGF
VEGF signaling
EC migration
EC proliferation
Sprouting angiogenesis
EC migration
Lymphocyte aggregation
Cell-cell adhesion (integrin)
Mucus secretion
Antigen presentation
T cell mediated cytotoxicity
- log10 (P-value)

526 **Figure 1: Adipose tissue shows an angiogenic gene profile in single-cell transcriptomics**
527 **among human stem cell sources**
528 (A) Workflow of scRNA-seq analysis to characterize pro/anti-angiogenic gene profiles of human
529 cell sources.
530 (B) tSNE map and clustering of 47,035 cells derived from BM, UCB, and AT (left). Distribution
531 of BM, UCB, and AT-Lin$^-$ cells (right).
532 (C) Heatmap with hierarchical clustering of gene expressions of 38 pro-/anti-angiogenic growth
533 factors in Lin$^-$ cells from human BM, UCB, and AT.
534 (D) Pathway enrichment analysis between indicated cell sources. The GO terms associated with
535 angiogenesis (red) or overrepresented on BM/UCB (blue) are displayed. See also **Figure S1**.

Figure 2

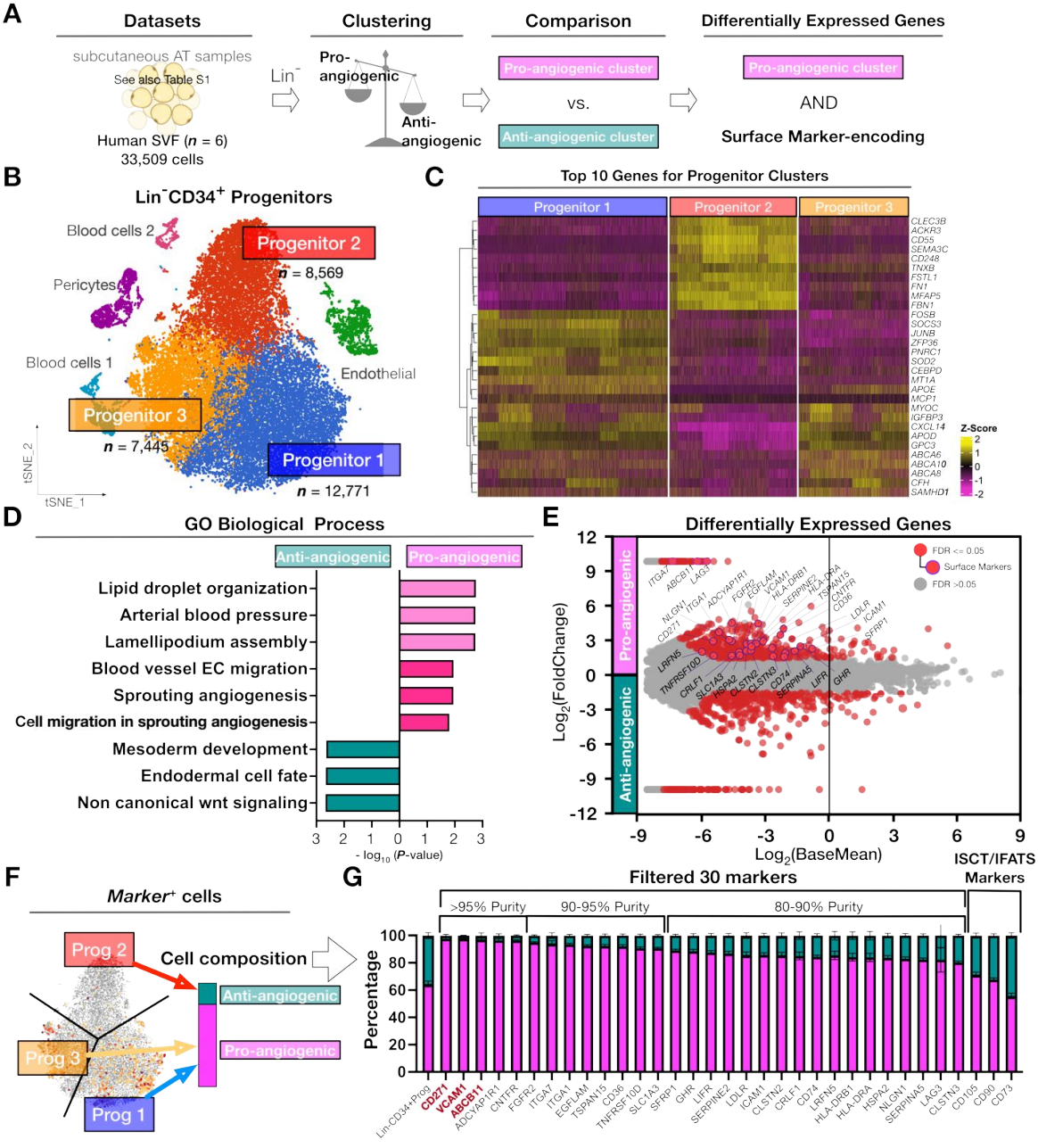
A
Datasets
subcutaneous AT samples
See also Table S1
Human SVF (n = 6)
33,509 cells
Clustering
Lin⁻
Pro-angiogenic
Anti-angiogenic
Comparison
Pro-angiogenic cluster
vs.
Anti-angiogenic cluster
Differentially Expressed Genes
Pro-angiogenic cluster
AND
Surface Marker-encoding
B
Lin⁻CD34⁺ Progenitors
Blood cells 2
Progenitor 2
n = 8,569
Pericytes
Blood cells 1
Endothelial
Progenitor 3
n = 7,445
Progenitor 1
n = 12,771
tSNE_2
tSNE_1
C
Top 10 Genes for Progenitor Clusters
Progenitor 1
Progenitor 2
Progenitor 3
Z-Score
D
GO Biological Process
Anti-angiogenic
Pro-angiogenic
Lipid droplet organization
Arterial blood pressure
Lamellipodium assembly
Blood vessel EC migration
Sprouting angiogenesis
Cell migration in sprouting angiogenesis
Mesoderm development
Endodermal cell fate
Non canonical wnt signaling
- log10 (P-value)
E
Differentially Expressed Genes
FDR <= 0.05
Surface Markers
FDR >0.05
Pro-angiogenic
Anti-angiogenic
Log2(FoldChange)
Log2(BaseMean)
F
Marker⁺ cells
Prog 2
Prog 3
Prog 1
Cell composition
Anti-angiogenic
Pro-angiogenic
G
Filtered 30 markers
>95% Purity
90-95% Purity
80-90% Purity
ISCT/IFATS Markers
Percentage
Lin-CD34+Prog
CD271
VCAM1
ABCB11
ADCYAP1R1
CNTFR
FGFR2
ITGA7
ITGA1
EGFLAM
TSPAN15
CD36
TNFRSF10D
SLC1A3
SFRP1
GHR
LIFR
SERPINE2
LDLR
ICAM1
CLSTN2
CRLF1
CD74
LRFN5
HLA-DRB1
HLA-DRA
HSPA2
NLGN1
SERPINA5
LAG3
CLSTN3
CD105
CD90
CD73

538 **Figure 2: Adipose tissue single-cell transcriptomics filters 30 surface markers of angiogenic**
539 **cluster cells**
540 (A) Diagram illustrating filtering strategy of surface marker genes specific for pro-angiogenic
541 cluster in human SVF.
542 (B) tSNE map and clustering of 33,509 SVF cells obtained from 6 human subcutaneous AT.
543 (C) Single-cell heatmap of top 10 marker gens among 3 progenitor clusters (***n*** = 6).
544 (D) Pathway enrichment analysis between pro-/anti-angiogenic clusters. The top 3
545 up/downregulated and angiogenesis-related GO terms are displayed (***n*** = 6).
546 (E) Volcano plot of 2,621 differentially expressed genes between pro/anti-angiogenic clusters.
547 Red dots show differentially expressed genes with $|\log_2(\text{FoldChange})| > 1.5$. Violet circles
548 highlight genes encoding surface proteins (***n*** = 6).
549 (F) Diagram illustrating the ranking analysis of 30 surface marker genes based on the purity of
550 pro-angiogenic cluster.
551 (G) Distribution of the pro/anti-angiogenic clusters within the surface marker expressing cell
552 populations (***n*** = 6). Data are presented as the mean ± SEM. See also **Figure S2**.

553 **Figure 3**

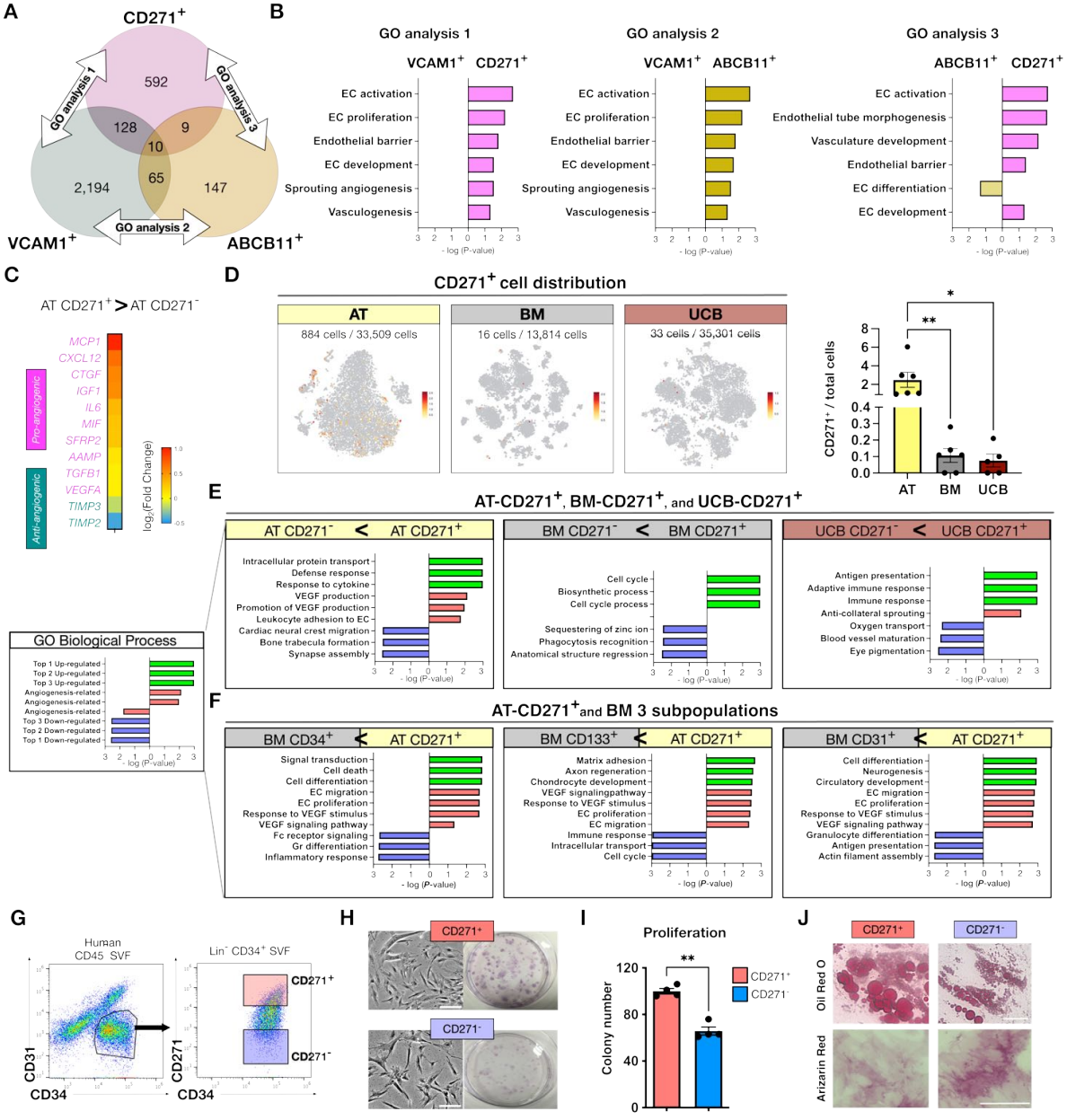

554

555 **Figure 3: Adipose tissue CD271$^+$ cell population is highly angiogenic**
556 (A) Venn diagram illustrating the overlap between CD271$^+$, VCAM1$^+$, and ABCB11$^+$ cells in
557 Lin$^-$CD34$^+$ progenitor cells in AT scRNAseq analysis (***n*** = 6).
558 (B) Pathway enrichment analysis between CD271$^+$, VCAM1$^+$, and ABCB11$^+$ cell populations.
559 (C) Heatmap of representative differentially expressed genes of pro-/anti-angiogenic factors
560 between CD271$^+$ and CD271$^-$ cells. The color shows the value of $\log_2$ Fold Change. (***n*** = 6).
561 (D) The distribution of CD271$^+$ cells in tSNE map and quantification of the frequency of
562 CD271$^+$ cells in AT, BM, and UCB (***n*** = 2/organ). The color of dot plots represents the
563 expression level of CD271.
564 (E) Pathway enrichment analysis between CD271$^+$ and CD271$^-$ cells in AT, BM, and UCB. The
565 top 3 up/downregulated and angiogenesis-associated GO terms are displayed (***n*** = 2/organ).
566 (F) Pathway enrichment analysis between AT-CD271$^+$ cells and three BM subpopulations. The
567 top 3 up/downregulated and angiogenesis-associated GO terms are displayed (***n*** = 2/organ).
568 (G) Representative flow cytometric plots from human subcutaneous AT SVF.
569 (H) Representative images of cultured ADSCs and generated colonies (Giemsa staining) in CFU
570 assay. Bars = 50 μm.
571 (I) Colony number in CFU assay of CD271$^+$ and CD271$^-$ ADSCs (***n*** = 4/group).
572 (J) Representative images of differentiation assays of CD271$^+$ and CD271$^-$ cells. Bars = 100 μm.
573 Data are presented as the mean ± SEM. ***P*** < 0.05 and ****P*** < 0.01.

Figure 4

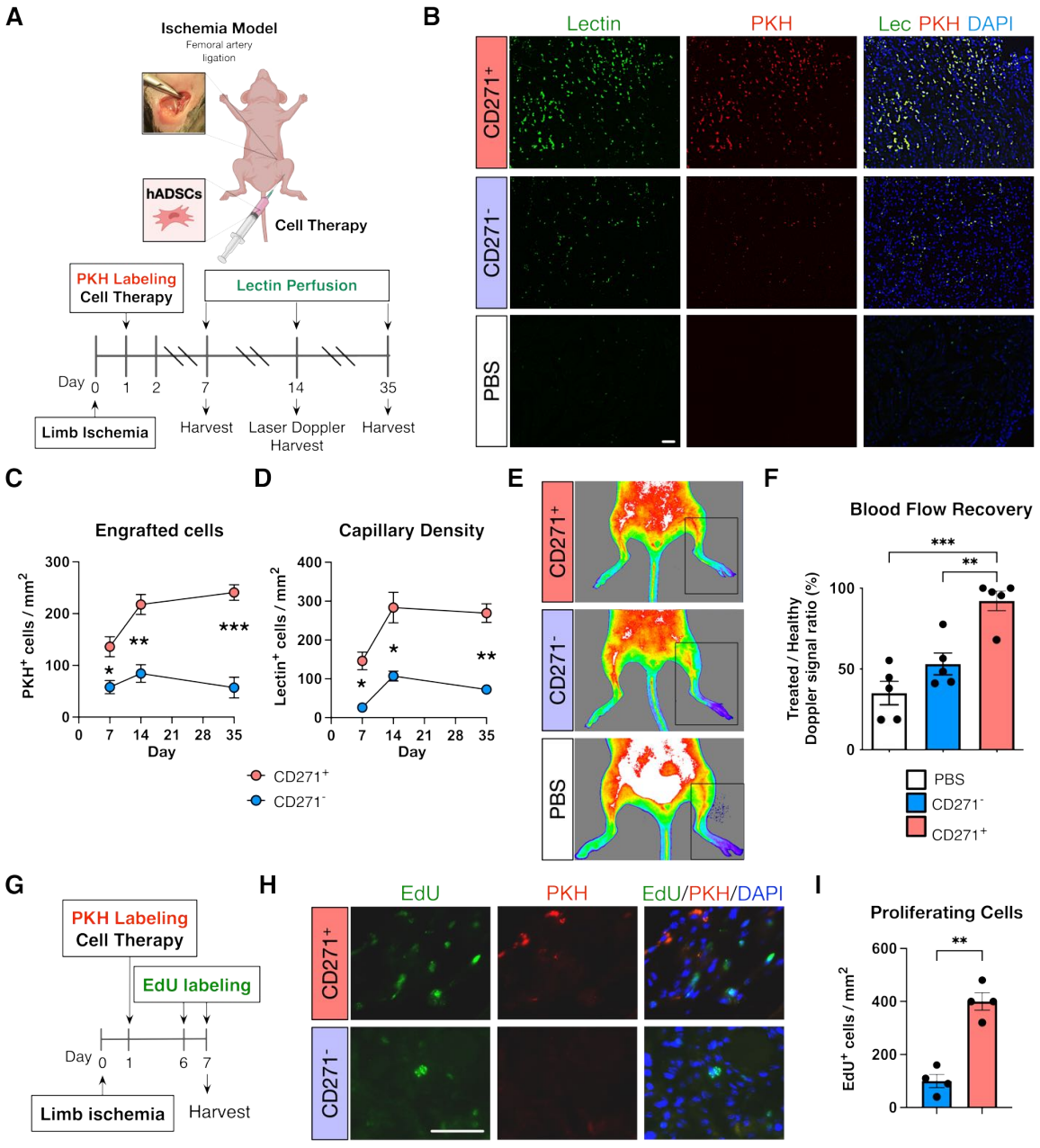
A
Ischemia Model
Femoral artery ligation
hADSCs
Cell Therapy
PKH Labeling Cell Therapy
Lectin Perfusion
Day 0 1 2 7 14 35
Limb Ischemia
Harvest
Laser Doppler Harvest
Harvest
B
Lectin
PKH
Lec PKH DAPI
CD271+
CD271-
PBS
C
Engrafted cells
PKH+ cells / mm2
Day
D
Capillary Density
Lectin+ cells / mm2
Day
CD271+
CD271-
E
CD271+
CD271-
PBS
F
Blood Flow Recovery
Treated / Healthy Doppler signal ratio (%)
PBS
CD271-
CD271+
G
PKH Labeling Cell Therapy
EdU labeling
Day 0 1 6 7
Limb ischemia
Harvest
H
EdU
PKH
EdU/PKH/DAPI
CD271+
CD271-
I
Proliferating Cells
EdU+ cells / mm2

576 **Figure 4: AT-CD271$^+$ progenitors have high *in vivo* angiogenic capacity with long-term**
577 **engraftment**
578 (A) Diagram of our cell therapy protocol using PKH-labeled human ADSCs and fluorescence-
579 conjugated lectin perfusion.
580 (B) Representative IHC images for lectin$^+$ capillaries and PKH$^+$ engrafted human ADSCs at day
581 14 after cell transplantation with either CD271$^+$ or CD271$^-$ progenitors. Bar = 100 μm.
582 (C) Quantitative analysis of engrafted ADSCs in ischemic limbs on day 7, 14, and 35 with either
583 CD271$^+$ or CD271$^-$ progenitors (***n*** = 5).
584 (D) Quantitative analysis of capillary density in ischemic limbs on day 7, 14, and 35 (***n*** = 5).
585 (E) Representative images of laser Doppler analysis at day 14 after cell therapy.
586 (F) Quantitative analysis of blood flow using laser Doppler analysis at day 14 after cell therapy
587 with either CD271$^+$ or CD271$^-$ progenitors. Signal of treated limb is normalized to signal from
588 healthy limb (set as 100%) (***n*** = 5).
589 (G) Diagram of cell therapy experiments to evaluate in vivo proliferating cells in ischemic limb
590 after cell therapy.
591 (H) Representative IHC images for EdU$^+$ cell nuclei and PKH$^+$ engrafted human CD271$^+$ or
592 CD271$^-$ progenitors at day 7 after cell therapy. Bar = 50 μm.
593 (I) Quantitative analysis of EdU$^+$ proliferating cells after CD271$^+$ or CD271$^-$ progenitor
594 treatment (***n*** = 4). Data are presented as the mean ± SEM. *$P < 0.05$, **$P < 0.01$ and ***$P <$
595 0.005. See also **Figure S3**.

Figure 5

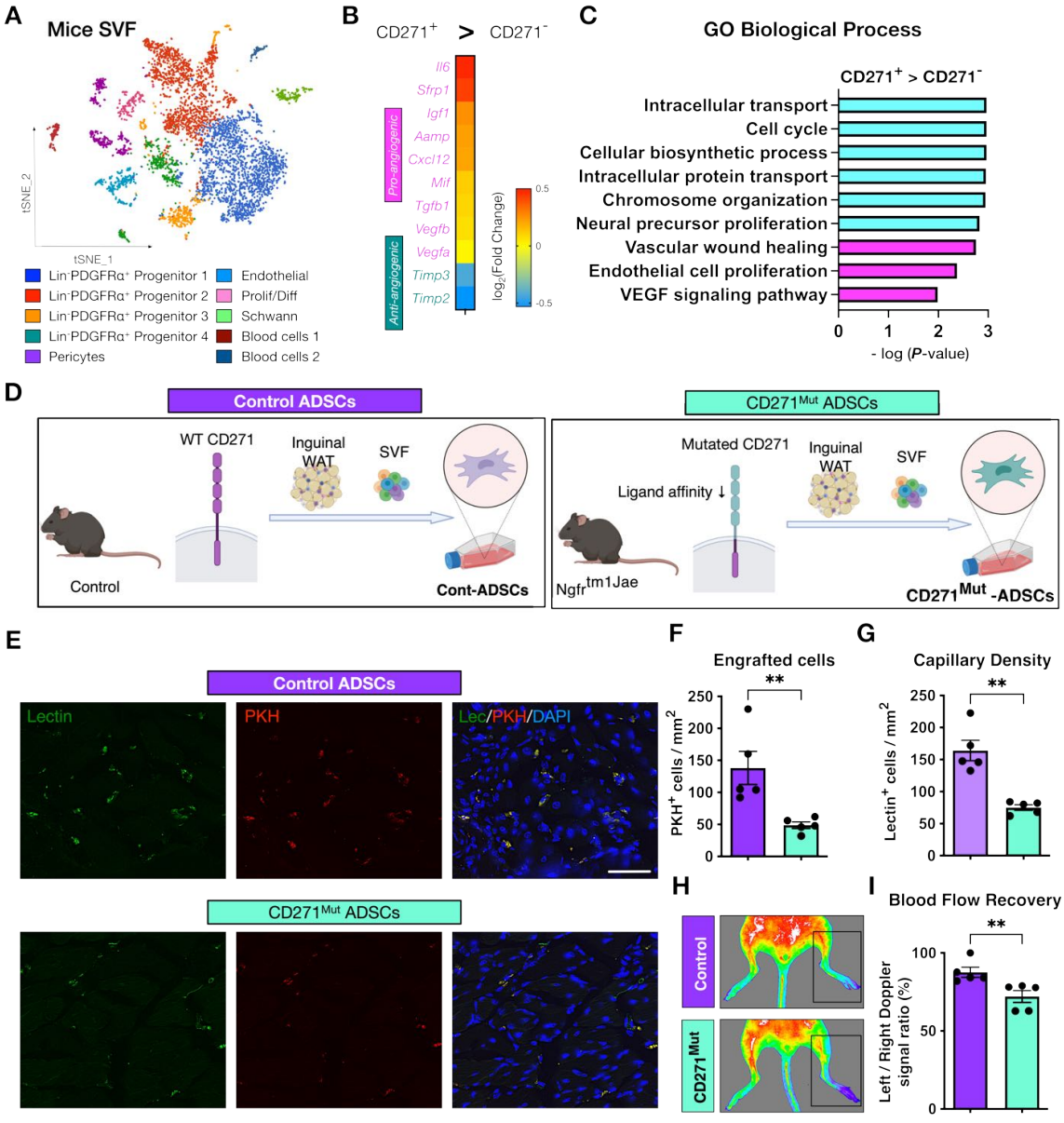
A
Mice SVF
tSNE_1
tSNE_2
Lin⁻PDGFRα⁺ Progenitor 1
Lin⁻PDGFRα⁺ Progenitor 2
Lin⁻PDGFRα⁺ Progenitor 3
Lin⁻PDGFRα⁺ Progenitor 4
Pericytes
Endothelial
Prolif/Diff
Schwann
Blood cells 1
Blood cells 2
B
CD271⁺ > CD271⁻
Il6
Sfrp1
Igf1
Aamp
Cxcl12
Mif
Tgfb1
Vegfb
Vegfa
Timp3
Timp2
Pro-angiogenic
Anti-angiogenic
log2(Fold Change)
0.5
0
-0.5
C
GO Biological Process
CD271⁺ > CD271⁻
Intracellular transport
Cell cycle
Cellular biosynthetic process
Intracellular protein transport
Chromosome organization
Neural precursor proliferation
Vascular wound healing
Endothelial cell proliferation
VEGF signaling pathway
0
1
2
3
- log (P-value)
D
Control ADSCs
WT CD271
Inguinal WAT
SVF
Control
Cont-ADSCs
CD271Mut ADSCs
Mutated CD271
Ligand affinity ↓
Inguinal WAT
SVF
Ngfrtm1Jae
CD271Mut -ADSCs
E
Control ADSCs
Lectin
PKH
Lec/PKH/DAPI
CD271Mut ADSCs
F
Engrafted cells
**
PKH⁺ cells / mm²
250
200
150
100
50
0
G
Capillary Density
**
Lectin⁺ cells / mm²
250
200
150
100
50
0
H
Control
CD271Mut
I
Blood Flow Recovery
**
Left / Right Doppler signal ratio (%)
100
50
0

598 **Figure 5: Normal CD271 activity is required for proangiogenic gene profile and *in vivo***
599 **angiogenic capacity of mouse ADSCs**
600 (A) tSNE map and clustering of 4,912 neonatal mouse inguinal fat pad SVF cells.
601 (B) Heatmap presentation of representative differentially expressed genes of pro/anti-angiogenic
602 factors between $CD271^+$ and $CD271^-$ mouse cells.
603 (C) Pathway enrichment analysis between mouse $CD271^+$ and $CD271^-$ mouse cells in Lin^-
604 $PDGFR\alpha^+$ progenitors. The top 6 upregulated and angiogenesis-associated GO terms are
605 displayed.
606 (D) Diagram illustrating preparation of CD271-mutated mouse-derived ($CD271^{Mut}$) and
607 littermate wild-type mouse-derived (Control) ADSCs.
608 (E) Representative IHC images of $lectin^+$ capillaries and PKH^+ engrafted mouse ADSCs on day
609 14 after cell transplantation with either $CD271^{Mut}$ or control ADSCs. Bar = 50 μm.
610 (F) Quantitative analysis of engrafted ADSCs in ischemic limbs on day 14 after treatment with
611 $CD271^{Mut}$ or control ADSCs. (***n***=5)
612 (G) Quantitative analysis of capillary density in ischemic limbs on day 14 after treatment with
613 $CD271^{Mut}$ or control ADSCs. (***n***=5)
614 (H) Representative images of laser Doppler analysis on day 14 after transplantation with
615 $CD271^{Mut}$ or control ADSCs following limb ischemia induction (***n*** = 5).
616 (I) Quantitative analysis of blood flow using laser Doppler analysis at day 14 after cell therapy
617 with either $CD271^{Mut}$ or control ADSCs. Signal of treated limb is normalized to signal from
618 healthy limb (set as 100%). Data are presented as the mean ± SEM. ***P*** < 0.05 and ****P*** < 0.01.
619 See also **Figure S4**.

Figure 6

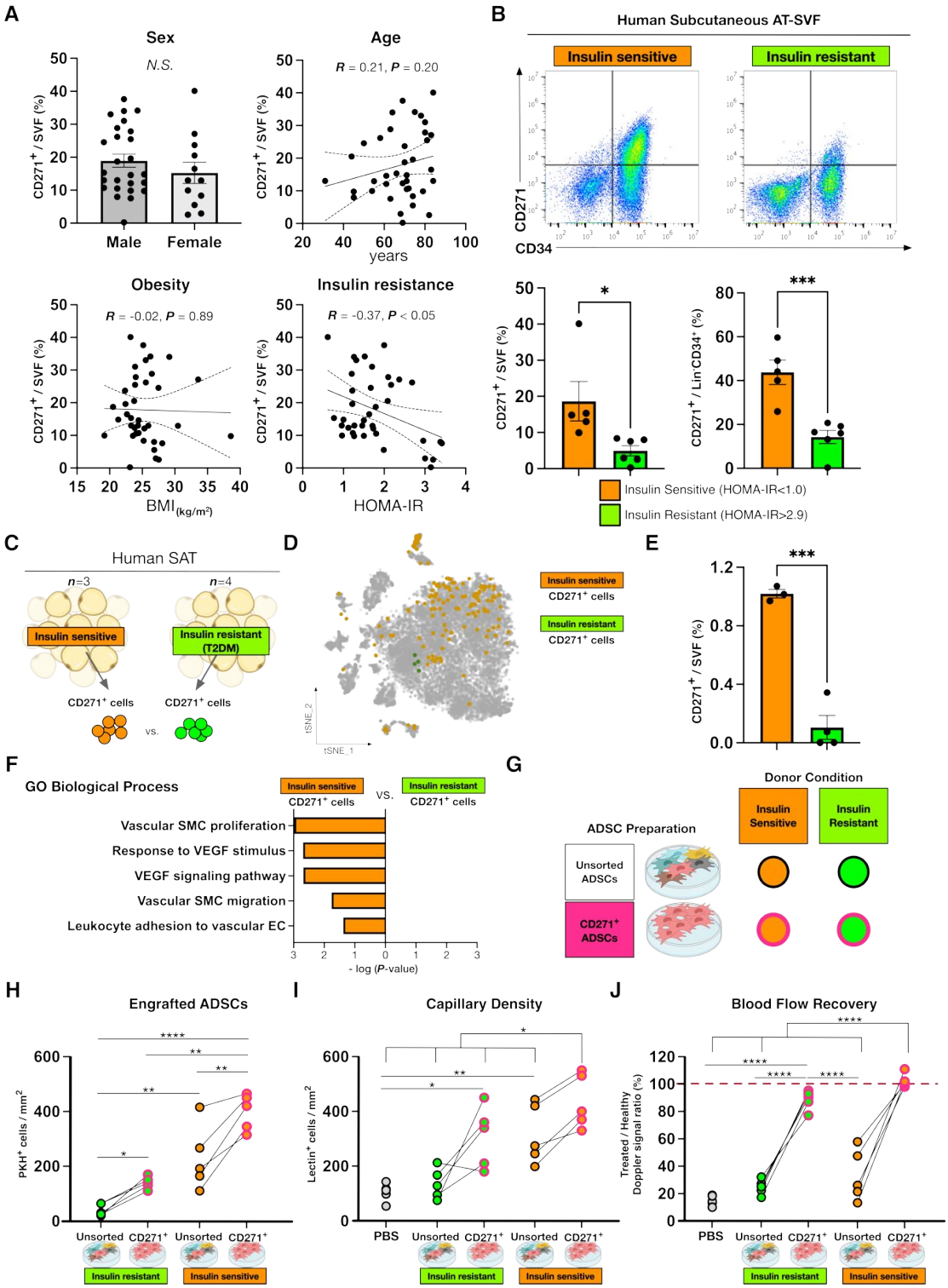
A
Sex
N.S.
CD271+ / SVF (%)
Male
Female
Age
R = 0.21, P = 0.20
years
Obesity
R = -0.02, P = 0.89
BMI (kg/m²)
Insulin resistance
R = -0.37, P < 0.05
HOMA-IR
B
Human Subcutaneous AT-SVF
Insulin sensitive
Insulin resistant
CD271
CD34
CD271+ / Lin-CD34+ (%)
Insulin Sensitive (HOMA-IR<1.0)
Insulin Resistant (HOMA-IR>2.9)
C
Human SAT
n=3
n=4
Insulin sensitive
Insulin resistant (T2DM)
CD271+ cells
vs.
D
tSNE_1
tSNE_2
E
F
GO Biological Process
Vascular SMC proliferation
Response to VEGF stimulus
VEGF signaling pathway
Vascular SMC migration
Leukocyte adhesion to vascular EC
- log (P-value)
G
Donor Condition
ADSC Preparation
Unsorted ADSCs
CD271+ ADSCs
H
Engrafted ADSCs
PKH+ cells / mm²
I
Capillary Density
Lectin+ cells / mm²
J
Blood Flow Recovery
Treated / Healthy Doppler signal ratio (%)
PBS
Unsorted
CD271+

622 **Figure 6: AT-CD271$^+$ progenitors are decreased and impaired in insulin resistant donors**
623 (A) Plots comparing CD271$^+$ cell frequency in SVF (CD271$^+$/SVF) and clinical parameters of
624 CVD patients with or without insulin resistance (***n*** = 38).
625 (B) Representative flow cytometric plots and comparative analysis of CD271$^+$ cell abundance in
626 total SVF or Lin$^-$CD34$^+$ SVF of CVD patients with or without insulin resistance (***n*** = 5-6).
627 (C) Diagram illustrating human AT samples used for scRNA-seq analysis
628 (D) Distribution of CD271$^+$ cells in tSNE map derived from lean healthy (***n*** = 3, insulin
629 sensitive, **blue dots**) and obese-diabetic patients (***n*** = 4, insulin resistant, **red dots**).
630 (E) Comparative analysis of the percentage of CD271$^+$ cells between patients with and without
631 insulin resistance in the scRNA-seq analysis (***n*** = 3-4).
632 (F) Pathway enrichment analysis between CD271$^+$ cells from patients with and without insulin
633 resistance. GO terms associated with angiogenesis are displayed.
634 (G) Diagram illustrating ADSC groups for cell therapy experiments stratified by donor types and
635 ADSC preparation methods (unsorted and CD271$^+$ ADSCs).
636 (H) Quantitative analysis of engrafted ADSCs and capillary density in ischemic limbs at day 14
637 after cell therapy (***n*** = 5). The red-colored dashed line indicates complete recovery of blood flow
638 (100%). *$P < 0.05$, **$P < 0.01$, ***$P < 0.005$, and ****$P < 0.001$. See also **Figure S6**.

Figure 7

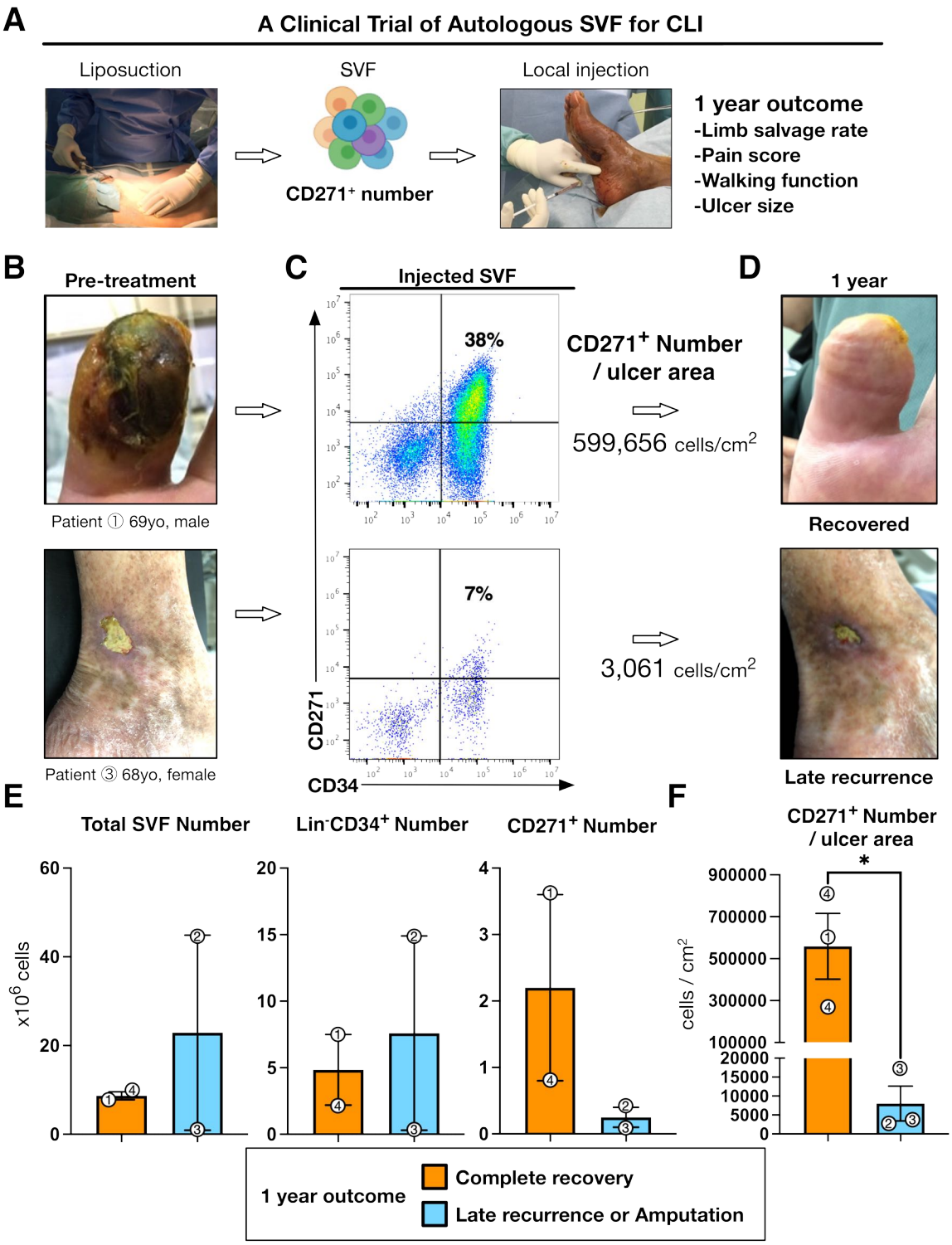
A
A Clinical Trial of Autologous SVF for CLI
Liposuction
SVF
Local injection
CD271+ number
1 year outcome
-Limb salvage rate
-Pain score
-Walking function
-Ulcer size
B
Pre-treatment
Patient ① 69yo, male
Patient ③ 68yo, female
C
Injected SVF
38%
7%
CD271
CD34
CD271+ Number / ulcer area
599,656 cells/cm2
3,061 cells/cm2
D
1 year
Recovered
Late recurrence
E
Total SVF Number
Lin-CD34+ Number
CD271+ Number
x10^6 cells
F
CD271+ Number / ulcer area
cells / cm2
*
1 year outcome
Complete recovery
Late recurrence or Amputation

641 **Figure 7: The number of AT-CD271$^+$ progenitors injected was significantly higher in**
642 **patients who completely recovered from CLI in SVF therapy**
643 (A) Diagram of the study design of a clinical trial of autologous SVF transplantation for CLI.
644 (B) Representative images of CLI lesions prior to autologous SVF transplantation.
645 (C) Representative flow cytometric analysis of autologous SVF transplantation.
646 (D) Representative images of CLI lesions acquired 12 months after autologous SVF
647 transplantation.
648 (E) Quantification of total SVF, Lin$^-$CD34$^+$, and CD271$^+$ cell numbers injected to CLI patients
649 (***n*** = 4)
650 (F) Quantification of the number of CD271$^+$ cells per ulcer area between patients (***n*** = 4 patients,
651 ***n*** = 6 ulcer lesions). Numbers within data point indicates patient identification number. Data are
652 represented as the mean ± SEM. ****P*** < 0.05. See also **Figure S7** and **Table S7**.

METHODS

RESOURCE AVAILABILITY

Lead contact

Further information and requests for resources and reagents will be fulfilled by the lead contact, Masayuki Takamura (mtakamura@staff.kanazawa-u.ac.jp)

Materials availability

None of unique reagents were generated in this study.

Data and code availability

Single-cell RNA-seq datasets analyzed in this study are available at NCBI Gene Expression Omnibus (GEO). GEO accession numbers are listed in **Table S1**. Any information and Seurat analysis files required to reanalyze the data reported in this study is available from the Lead Contact upon request.

EXPERIMENTAL MODEL AND SUBJECT DETAILS

Study Design and Patient Population

In the study of patient-derived AT and SVF, eligible patients were adult males or females with CVD who underwent elective cardiac surgery, including coronary artery bypass grafting (CABG) and cardiac valve replacement/plastic surgeries. Major exclusion criteria were acute emergency diseases, including acute myocardial infarction, active and acute infectious disease, uncontrolled diabetes mellitus (HbA1c > 8.0%), hypo/hyperinsulinemia (< 2.2 or > 13.0 μU/mL), systemic inflammatory disease (autoimmune disease), and history of irradiation therapy at tissue harvest sites. Thirty-eight patients were enrolled between April 2017 and February 2022. This study was registered in the University Hospital Medical Information Network Center (UMIN, Tokyo, Japan) Clinical Trials Registration System as UMIN000020764. After enrollment with written informed consent, clinical and laboratory variables were collected preoperatively, and all data were blinded for the researchers who performed further experiments.

The detailed protocol and eligibility for the clinical trial of SVF therapy for CLI are published,[47,67] Briefly, this was a multicenter clinical trial (UMIN000010143) to investigate the feasibility and safety of SVF injection for CLI patients with no option for treatment[47].

Autologous SVF from liposuction was transplanted to the ulcer lesions via intra-muscular injections. The safety, feasibility, and the efficacy including hard outcomes, including survival rate and amputation free rate in 6 months, of SVF therapy were investigated. In this study, we sub-analyzed 4 patients (**Table S6**) on whom we performed cell therapy in our institution (Kanazawa University) with 1-year follow-up data. On the remaining samples after SVF injection, we analyzed their viability and surface antigen expressions.

The studies using human samples subjects was performed according to Declaration of Helsinki principles and approved by the Research Ethics Board of the University of Kanazawa. Written informed consent was obtained from all patients prior to inclusion in the study. All animal experiments were approved by the Institution for Experimental Animals of the Kanazawa University Advanced Science Research Center.

Mice

All animal protocols were approved and performed according to the Guide for the Care and Use of Laboratory Animals of Kanazawa University, which strictly conforms to the Guide for the Care and Use of Laboratory Animals published by the US National Institutes of Health (NIH, Bethesda, MD, USA). Athymic nude mice for xenograft experiments were purchased from the Charles River Laboratories. Heterozygous $Ngfr^{tm1jae42}$ were purchased from the Jackson Laboratory (Strain #002213) and crossed two- or three-times with C57BL/6J females before generating homozygous $Ngfr^{tm1Jae}$ ($CD271^{Mut}$) mice. Homozygous $Ngfr^{tm1Jae}$ and controls mice were used at 6–8-week-old) before they develop peripheral nervous denervation and cutaneous ulcers (16 weeks old).

Cell Therapy Model of Limb Ischemia

6- to 8-week-old athymic nude mice (Jackson Laboratory) were subjected to hindlimb ischemia. Mice were anesthetized by intraperitoneal injection of sodium pentobarbital (40 mg/kg). The proximal portion of the left femoral artery was resected. After 24 h, 0.5 million human ADSCs at passage 4-6 were prepared for injection. In brief, ADSCs were harvested by trypsinization, labeled with PKH26 cell linker dye (2 μL/mL, 3 minutes in room temperature, Sigma), and resuspended in PBS (5.0×10^5 cells in 60 μl with 27 gauge syringes). Labeled ADSCs were immediately injected intra-muscularly at three different sites (gastrocnemius, gracilis, and quadriceps muscles, 20 μl per injection). Sham-operated mice were injected with PBS and used as a control group. At day 7, 14, and 35 after cell therapy, mice were anesthetized and subjected to laser Doppler analysis for blood flow, followed by harvest of gastrocnemius muscles.

713 **METHOD DETAILS**

714 **Single-Cell Transcriptome Datasets and Analysis**

715 We used scRNA-seq datasets of AT,[26,68,69] BM,[24,70] and UCB.[25,71] Gene Expression Omnibus
716 (GEO) accession numbers of revisited datasets are listed in **Table S1**. For quality control, cells
717 expressing < 200 genes and with a mitochondrial content > 5% were removed. For batch
718 integration of multiple scRNAseq datasets, Harmony was used to remove the batch effect.[72] After
719 data normalization, dimension reduction (tSNE) and clustering with using a Louvain algorism
720 were performed. Marker gene analysis and differential expression (DE) analysis were performed
721 using non-parametric approach, Venice[73] or DESeq2. The Gene Set Enrichment Analysis
722 (GSEA) was performed to list GO Biological Process terms.[74] Cluster annotation was determined
723 according to marker genes for clusters identified by non-parametric approach, Venice and
724 collation with overlapping genes from the Human Cell Atlas and previously published scRNA-
725 seq reports.[19,21] These analyses were performed in BioTuring Browser 3.[75]

726 **Adipose Tissue and SVF Processing**

727 Unnecessary subcutaneous adipose tissues (1-2 gram) discarded during making surgical incision
728 were obtained. SVF cells were isolated from adipose tissue using a procedure modified from Zuk
729 et al.[39] Briefly, adipose tissue was digested by Liberase TM Research Grade collagenase solution
730 (0.4 units/mL; Sigma-Aldrich) for 30 min using gentleMACS Dissociator ("ATDK" program,
731 Miltenyi Biotec). Then, the digested solution was filtered through a 100-µm cell strainer (BD
732 Biosciences) to remove undigested connective tissue debris. After centrifugation (400g, 10
733 minutes at room temperature), the supernatant containing mature adipocytes was discarded. The
734 pellet was lysed to deplete erythrocytes with BD Pharm Lyse (2mL for 1 minute at room
735 temperature, BD Biosciences) and washed twice with phosphate-buffered saline (PBS) with
736 2.0% fetal bovine serum (FBS). The final pellet was resuspended in 150 μL of autoMACS
737 Running buffer (Miltenyi) and counted with a hemocytometer in triplicate.

738 **Flow Cytometry and Sorting**

739 SVF cells were separated into $CD45^+$ and $CD45^-$ cells using microbeads and autoMACS pro
740 separator (Miltenyi) according to the manufacturer's instructions. $CD45^-$ cells were incubated
741 with Fc Block (BD Biosciences) prior to staining. Then, cells were labeled with following
742 antibodies: human CD31-FITC (BD Biosciences, clone WM59, used in 1:20 dilution), CD271-
743 APC (Miltenyi, cloneME20.4-1.H4, 1:20), and CD34-peridinin chlorophyll protein (PerCP) (BD
744 Biosciences, clone 8G12, 1:20) for 15 min at 4°C. Then, cells were washed twice in PBS with

745 2.0% FBS. Flow cytometric data were acquired by using Accuri C6 (BD Biosciences). Before
746 immunophenotyping, the instrument performance was validated by using BD Accuri Spherotech
747 Validation Beads (BD Biosciences). A total of 30,000-100,000 events were acquired at slow flow
748 rate. Acquired data were analyzed using FlowJo software X 10.0.7 (Tree Star Inc.). Isotype-
749 matched negative controls or fluorescence-minus controls were used to define the threshold for
750 each specific signal and establish the appropriate gate for positive cells.

751 **Cell Culture**

752 The $CD45^-$ stromal cells that remained from flow cytometric analysis were seeded at a density of
753 1.0×10^4 cells/cm^2. Cells were cultured in standard conditions (5% carbon dioxide, 37°C) in
754 DMEM/F12 (Thermo Fisher Scientific) supplemented with 10% FBS and 1% antibiotic-
755 antimycotic (Thermo Fisher Scientific) solution. At 24 h after seeding, non-adherent cells were
756 removed by washing the plates, and then medium was changed every three days. ADSCs were
757 harvested at sub-confluency with trypsin (0.05% trypsin-EDTA; Thermo Fisher Scientific). Cells
758 at the second passage and thereafter were replated at a density of 3,000 cells/cm2.

759 **RT-qPCR**

760 Total RNA was isolated from ADSCs using RNeasy Mini Kit (Qiagen). Total RNA (100 ng) was
761 used to generate cDNA using the TaqMan Universal Master Mix (Applied Biosystems).
762 Quantitative real-time polymerase chain reaction (qRT-PCR) analysis was performed on an ABI
763 Prism 7300 sequence detection system (Applied Biosystems). The TaqMan probes (Applied
764 Biosystems) used in this study were listed in **Table S7**. Relative expression was assessed by
765 comparative CT method, correcting for amplification efficiency of the primers, and performed in
766 duplicate.

767 **Colony-Forming Unit Assay**

768 Cultured AT-$CD271^+$ or $CD271^-$ progenitors at passage 4 were used for colony-forming unit
769 (CFU) assays. Cells were detached and plated at a density of 20 cells/cm^2 in 10 cm dishes. Half
770 the medium was changed at day 7 after plating. Adherent cell clusters of greater than 50 cells
771 were counted at day 14 with Giemsa staining. The experiments were performed in triplicate for
772 each sample.

773 **Flow Cytometry of ADSC treated limb**

774 At 14 days after cell therapy in xenograft model, gastrocnemius muscle was harvested and
775 digested using gentleMACS (Miltenyi) with "m_muscle_01" program and Liberase TM solution.
776 Single cells from digested limb were filtered through 40 μ m cell strainer and labeled with

777 immunofluorescence-conjugated antibodies; mice CD31-PerCP-Cy$^{5.5}$ (BD Bioscience, clone
778 MEC 13.3, 1:20), human CD31-FITC (BD Biosciences, clone WM59), human CD271-APC
779 (Miltenyi, cloneME20.4-1.H4, 1:20), human CD90-APC (BD Biosciences, clone 5E10), and
780 human CD105-PerCP-Cy$^{5.5}$ (BD Biosciences, clone 266, 1:20) for 15 min at 4°C. Flow
781 cytometric data was acquired by similar methods described above in *Flow Cytometry and*
782 *Sorting* section.

783 **Blood Flow Measurement**

784 Blood flow was assessed using Laser Doppler blood flow imager (OZ-2 LCB, OMEGAWAVE,
785 Japan) at day 1, 3, and 14 after induction of limb ischemia. Before scanning, mice were placed
786 on a heating plate at 37°C for 15 min, followed by anesthetization using intraperitoneal injection
787 of sodium pentobarbital (20 mg/kg). The signal intensities basically reflecting laser scattering by
788 red blood cells within circulation were obtained as blood flow value. The mean blood flow value
789 was acquired in region of interest (ROI) capturing the whole mouse lower limb. The ratio of
790 blood flow values of the ischemic (left) limb to the healthy (right) limb were calculated as blood
791 flow recovery to avoid data variations caused by ambient light and temperature.[8,9]

792 **In Vivo Proliferation Assay**

793 EdU solution (5mg/2mL) was administered via intra-peritoneal injection at day 6 after ADSC
794 therapy. At day 7, the gastrocnemius muscles were harvested and processed to frozen sections.
795 EdU positive nucleus were detected using EdU *in vivo* imaging kits (BCK488-IV-IM, baseclick)
796 according to the manufacturer's instruction. The number of EdU^{+} and DAPI^{+} nucleus was
797 counted in frozen sections in duplicate.

798 **Immunohistochemistry**

799 Tissue vascularization and ADSCs engraftment were evaluated at day 14 and 35. Mice were
800 anesthetized and injected with 50 μg of FITC-conjugated isolectin B4 (FL-1201, Vector
801 Laboratories) via tail vein. After 10 min, mice were perfused with PBS for 3 min to remove
802 unbound isolectin B4 in the blood vessels, and perfusion-fixed with 4% paraformaldehyde. The
803 gastrocnemius muscles were removed, fixed with 4% paraformaldehyde at 4°C overnight, and
804 incubated in 30% sucrose solution for 24 hours. Frozen sections of the tissue were obtained at 10
805 μm thickness and counterstained with DAPI. Capillary density and engraftment of injected
806 ADSCs were analyzed by counting FITC and PKH positive cells, respectively, in five randomly
807 selected fields per section. The experiments were performed in duplicate or triplicate for each
808 human ADSCs sample.

809 **Statistics**

810 Continuous data are expressed as the mean ± SEM, and statistical analysis was performed with
811 Prism 9 software (GraphPad, USA). Group comparisons were performed using paired or
812 unpaired *t* tests or one-way analysis of variance (ANOVA). Correlation analysis was performed
813 using Pearson correlation for normally distributed data (Shapiro–Wilk normality test) or
814 Spearman correlation for nonnormally distributed data. Statistical significance was defined as $^{*}\boldsymbol{P}$
815 < 0.05, $^{**}\boldsymbol{P} < 0.01$, $^{***}\boldsymbol{P} < 0.005$ and $^{****}\boldsymbol{P} < 0.001$. All reported statistical tests were two-
816 tailed.

REFERENCES

1. Roth, G.A., Johnson, C., Abajobir, A., Abd-Allah, F., Abera, S.F., Abyu, G., Ahmed, M., Aksut, B., Alam, T., Alam, K., et al. (2017). Global, Regional, and National Burden of Cardiovascular Diseases for 10 Causes, 1990 to 2015. Journal of the American College of Cardiology *70*, 1-25. 10.1016/j.jacc.2017.04.052.
2. Norgren, L., Hiatt, W.R., Dormandy, J.A., Nehler, M.R., Harris, K.A., Fowkes, F.G., and Rutherford, R.B. (2007). Inter-society consensus for the management of peripheral arterial disease. International angiology : a journal of the International Union of Angiology *26*, 81-157. 10.1016/j.jvs.2006.12.037.
3. Lawall, H., Bramlage, P., and Amann, B. (2011). Treatment of peripheral arterial disease using stem and progenitor cell therapy. Journal of Vascular Surgery *53*, 445-453. 10.1016/j.jvs.2010.08.060.
4. Annex, B.H. (2013). Therapeutic angiogenesis for critical limb ischaemia. Nature Reviews Cardiology *10*, 387-396. 10.1038/nrcardio.2013.70.
5. Samsonraj, R.M., Raghunath, M., Nurcombe, V., Hui, J.H., van Wijnen, A.J., and Cool, S.M. (2017). Concise Review: Multifaceted Characterization of Human Mesenchymal Stem Cells for Use in Regenerative Medicine. Stem Cells Translational Medicine *6*, 2173-2185. 10.1002/sctm.17-0129.
6. Gnecchi, M., Zhang, Z., Ni, A., and Dzau, V.J. (2008). Paracrine mechanisms in adult stem cell signaling and therapy. Circ Res *103*, 1204-1219. 10.1161/circresaha.108.176826.
7. Qadura, M., Terenzi, D.C., Verma, S., Al-Omran, M., and Hess, D.A. (2018). Concise Review: Cell Therapy for Critical Limb Ischemia: An Integrated Review of Preclinical and Clinical Studies. Stem Cells, 161-171. 10.1002/stem.2751.
8. Miranville, A. (2004). Improvement of Postnatal Neovascularization by Human Adipose Tissue-Derived Stem Cells. Circulation *110*, 349-355. 10.1161/01.CIR.0000135466.16823.D0.
9. Barros, S.D., Dehez, S., Arnaud, E., Barreau, C., Cazavet, A., Perez, G., Galinier, A., Casteilla, L., and Planat-Bénard, V. (2013). Aging-related Decrease of Human ASC Angiogenic Potential Is Reversed by Hypoxia Preconditioning Through ROS Production. Molecular Therapy *21*, 399-408. 10.1038/mt.2012.213.
10. Beltrán-Camacho, L., Rojas-Torres, M., and Durán-Ruiz, M.C. (2021). Current status of angiogenic cell therapy and related strategies applied in critical limb ischemia. International Journal of Molecular Sciences *22*, 1-27. 10.3390/ijms22052335.
11. Kim, H., Cho, H.-J., Kim, S.-W., Liu, B., Choi, Y.J., Lee, J., Sohn, Y.-D., Lee, M.-Y., Houge, M.a., and Yoon, Y.-s. (2010). CD31+ cells represent highly angiogenic and vasculogenic cells in bone marrow: novel role of nonendothelial CD31+ cells in neovascularization and their therapeutic effects on ischemic vascular disease. Circulation research *107*, 602-614. 10.1161/CIRCRESAHA.110.218396.
12. Rigato, M., Monami, M., and Fadini, G.P. (2017). Autologous Cell Therapy for Peripheral Arterial Disease. Circulation Research *120*, 1326-1340. doi:10.1161/CIRCRESAHA.116.309045.
13. Chiang, K.J., Chiu, L.C., Kang, Y.N., and Chen, C. (2021). Autologous stem cell therapy for chronic lower

852 extremity wounds: A meta-analysis of randomized controlled trials. Cells *10*, 1-17. 10.3390/cells10123307.
853 14. Losordo, D.W., Kibbe, M.R., Mendelsohn, F., Marston, W., Driver, V.R., Sharafuddin, M., Teodorescu, V.,
854 Wiechmann, B.N., Thompson, C., Kraiss, L., et al. (2012). A randomized, controlled pilot study of
855 autologous CD34+ cell therapy for critical limb ischemia. Circulation: Cardiovascular Interventions *5*, 821-
856 830. 10.1161/CIRCINTERVENTIONS.112.968321.
857 15. Fang, Y., Wei, Z., Chen, B., Pan, T., Gu, S., Liu, P., Guo, D., Xu, X., Jiang, J., Yang, J., et al. (2018). A
858 Five-Year Study of the Efficacy of Purified CD34+ Cell Therapy for Angiitis-Induced No-Option Critical
859 Limb Ischemia. STEM CELLS Translational Medicine *7*, 583-590. 10.1002/sctm.17-0252.
860 16. Raval, A.N., Schmuck, E.G., Tefera, G., Leitzke, C., Ark, C.V., Hei, D., Centanni, J.M., de Silva, R., Koch,
861 J., Chappell, R.G., and Hematti, P. (2014). Bilateral administration of autologous CD133+ cells in
862 ambulatory patients with refractory critical limb ischemia: lessons learned from a pilot randomized, double-
863 blind, placebo-controlled trial. Cytotherapy *16*, 1720-1732. 10.1016/j.jcyt.2014.07.011.
864 17. Etzrodt, M., Endele, M., and Schroeder, T. (2014). Quantitative single-cell approaches to stem cell research.
865 Cell Stem Cell *15*, 546-558. 10.1016/j.stem.2014.10.015.
866 18. Wilson, N.K., Kent, D.G., Buettner, F., Shehata, M., Macaulay, I.C., Calero-Nieto, F.J., Sánchez Castillo,
867 M., Oedekoven, C.A., Diamanti, E., Schulte, R., et al. (2015). Combined Single-Cell Functional and Gene
868 Expression Analysis Resolves Heterogeneity within Stem Cell Populations. Cell Stem Cell *16*, 712-724.
869 10.1016/j.stem.2015.04.004.
870 19. Han, X., Zhou, Z., Fei, L., Sun, H., Wang, R., Chen, Y., Chen, H., Wang, J., Tang, H., Ge, W., et al. (2020).
871 Construction of a human cell landscape at single-cell level. Nature *581*, 303-309. 10.1038/s41586-020-
872 2157-4.
873 20. Sun, W., Dong, H., Balaz, M., Slyper, M., Drokhlyansky, E., Colleluori, G., Giordano, A., Kovanicova, Z.,
874 Stefanicka, P., Balazova, L., et al. (2020). snRNA-seq reveals a subpopulation of adipocytes that regulates
875 thermogenesis. Nature *587*, 98-102. 10.1038/s41586-020-2856-x.
876 21. Emont, M.P., Jacobs, C., Essene, A.L., Pant, D., Tenen, D., Colleluori, G., Di Vincenzo, A., Jørgensen,
877 A.M., Dashti, H., Stefek, A., et al. (2022). A single-cell atlas of human and mouse white adipose tissue.
878 Nature. 10.1038/s41586-022-04518-2.
879 22. Deng, Q., Han, G., Puebla-Osorio, N., Ma, M.C.J., Strati, P., Chasen, B., Dai, E., Dang, M., Jain, N., Yang,
880 H., et al. (2020). Characteristics of anti-CD19 CAR T cell infusion products associated with efficacy and
881 toxicity in patients with large B cell lymphomas. Nature Medicine *26*, 1878-1887. 10.1038/s41591-020-
882 1061-7.
883 23. Rabilloud, T., Potier, D., Pankaew, S., Nozais, M., Loosveld, M., and Payet-Bornet, D. (2021). Single-cell
884 profiling identifies pre-existing CD19-negative subclones in a B-ALL patient with CD19-negative relapse
885 after CAR-T therapy. Nature Communications *12*, 865. 10.1038/s41467-021-21168-6.
886 24. Muto, T., Guillamot, M., Yeung, J., Fang, J., Bennett, J., Nadorp, B., Lasry, A., Redondo, L.Z., Choi, K.,
887 Gong, Y., et al. (2022). TRAF6 functions as a tumor suppressor in myeloid malignancies by directly

888 targeting MYC oncogenic activity. Cell Stem Cell *29*, 298-314.e299. 10.1016/j.stem.2021.12.007.
889 25. Luo, O.J., Lei, W., Zhu, G., Ren, Z., Xu, Y., Xiao, C., Zhang, H., Cai, J., Luo, Z., Gao, L., et al. (2022).
890 Multidimensional single-cell analysis of human peripheral blood reveals characteristic features of the
891 immune system landscape in aging and frailty. Nature Aging *2*, 348-364. 10.1038/s43587-022-00198-9.
892 26. Hildreth, A.D., Ma, F., Wong, Y.Y., Sun, R., Pellegrini, M., and O'Sullivan, T.E. (2021). Single-cell
893 sequencing of human white adipose tissue identifies new cell states in health and obesity. Nat Immunol *22*,
894 639-653. 10.1038/s41590-021-00922-4.
895 27. He, S., Wang, L.-H., Liu, Y., Li, Y.-Q., Chen, H.-T., Xu, J.-H., Peng, W., Lin, G.-W., Wei, P.-P., Li, B., et al.
896 (2020). Single-cell transcriptome profiling of an adult human cell atlas of 15 major organs. Genome
897 Biology *21*, 294. 10.1186/s13059-020-02210-0.
898 28. Karlsson, M., Zhang, C., Méar, L., Zhong, W., Digre, A., Katona, B., Sjöstedt, E., Butler, L., Odeberg, J.,
899 Dusart, P., et al. (2021). A single–cell type transcriptomics map of human tissues. Science
900 Advances *7*, eabh2169. doi:10.1126/sciadv.abh2169.
901 29. Banas, A., Teratani, T., Yamamoto, Y., Tokuhara, M., Takeshita, F., Osaki, M., Kawamata, M., Kato, T.,
902 Okochi, H., and Ochiya, T. (2008). IFATS collection: in vivo therapeutic potential of human adipose tissue
903 mesenchymal stem cells after transplantation into mice with liver injury. Stem cells (Dayton, Ohio) *26*,
904 2705-2712. 10.1634/stemcells.2008-0034.
905 30. Kim, H., Cho, H.J., Kim, S.W., Liu, B., Choi, Y.J., Lee, J., Sohn, Y.D., Lee, M.Y., Houge, M.A., and Yoon,
906 Y.S. (2010). CD31+ cells represent highly angiogenic and vasculogenic cells in bone marrow: Novel role of
907 nonendothelial CD31+ cells in neovascularization and their therapeutic effects on ischemic vascular
908 disease. Circulation Research *107*, 602-614. 10.1161/CIRCRESAHA.110.218396.
909 31. Gincberg, G., Shohami, E., Lazarovici, P., and Elchalal, U. (2018). Human Umbilical Cord Blood CD45(+)
910 Pan-Hematopoietic Cells Induced a Neurotherapeutic Effect in Mice with Traumatic Brain Injury:
911 Immunophenotyping, Comparison of Maternal and Neonatal Parameters, and Immunomodulation. J Mol
912 Neurosci *64*, 185-199. 10.1007/s12031-017-1008-8.
913 32. Ratajczak, M.Z., Kucia, M., Jadczyk, T., Greco, N.J., Wojakowski, W., Tendera, M., and Ratajczak, J.
914 (2012). Pivotal role of paracrine effects in stem cell therapies in regenerative medicine: can we translate
915 stem cell-secreted paracrine factors and microvesicles into better therapeutic strategies? Leukemia *26*,
916 1166-1173. 10.1038/leu.2011.389.
917 33. Xu, L., Kanasaki, K., Kitada, M., and Koya, D. (2012). Diabetic angiopathy and angiogenic defects.
918 Fibrogenesis & Tissue Repair *5*, 13. 10.1186/1755-1536-5-13.
919 34. Logsdon, E.A., Finley, S.D., Popel, A.S., and Gabhann, F.M. (2014). A systems biology view of blood
920 vessel growth and remodelling. Journal of Cellular and Molecular Medicine *18*, 1491-1508.
921 https://doi.org/10.1111/jcmm.12164.
922 35. Madu, C.O., Wang, S., Madu, C.O., and Lu, Y. (2020). Angiogenesis in Breast Cancer Progression,
923 Diagnosis, and Treatment. Journal of Cancer *11*, 4474-4494. 10.7150/jca.44313.

36. Traktuev, D.O., Merfeld-Clauss, S., Li, J., Kolonin, M., Arap, W., Pasqualini, R., Johnstone, B.H., and March, K.L. (2008). A population of multipotent CD34-positive adipose stromal cells share pericyte and mesenchymal surface markers, reside in a periendothelial location, and stabilize endothelial networks. Circulation Research *102*, 77-85. 10.1161/CIRCRESAHA.107.159475.

37. Bourin, P., Bunnell, B.a., Casteilla, L., Dominici, M., Katz, A.J., March, K.L., Redl, H., Rubin, J.P., Yoshimura, K., and Gimble, J.M. (2013). Stromal cells from the adipose tissue-derived stromal vascular fraction and culture expanded adipose tissue-derived stromal/stem cells: A joint statement of the International Federation for Adipose Therapeutics and Science (IFATS) and the International So. Cytotherapy *15*, 641-648. 10.1016/j.jcyt.2013.02.006.

38. Mabuchi, Y., Morikawa, S., Harada, S., Niibe, K., Suzuki, S., Renault-Mihara, F., Houlihan, D.D., Akazawa, C., Okano, H., and Matsuzaki, Y. (2013). LNGFR+THY-1+VCAM-1hi+ Cells Reveal Functionally Distinct Subpopulations in Mesenchymal Stem Cells. Stem Cell Reports *1*, 152-165. 10.1016/j.stemcr.2013.06.001.

39. Zuk, P.A., Zhu, M., and Ashjian, P. (2002). Human adipose tissue is a source of multipotent stem cells. Molecular biology of the cell *13*, 4279-4295. 10.1091/mbc.E02.

40. Sengenès, C., Miranville, A., Maumus, M., de Barros, S., Busse, R., and Bouloumié, A. (2007). Chemotaxis and differentiation of human adipose tissue CD34+/CD31- progenitor cells: role of stromal derived factor-1 released by adipose tissue capillary endothelial cells. Stem cells (Dayton, Ohio) *25*, 2269-2276. 10.1634/stemcells.2007-0180.

41. Rondini, E.A., Ramseyer, V.D., Burl, R.B., Pique-Regi, R., and Granneman, J.G. (2021). Single cell functional genomics reveals plasticity of subcutaneous white adipose tissue (WAT) during early postnatal development. Molecular Metabolism *53*, 101307. https://doi.org/10.1016/j.molmet.2021.101307.

42. Lee, K.F., Li, E., Huber, L.J., Landis, S.C., Sharpe, A.H., Chao, M.V., and Jaenisch, R. (1992). Targeted mutation of the gene encoding the low affinity NGF receptor p75 leads to deficits in the peripheral sensory nervous system. Cell *69*, 737-749. 10.1016/0092-8674(92)90286-L.

43. Chao, M.V. (2003). Neurotrophins and their receptors: A convergence point for many signalling pathways. Nature Reviews Neuroscience *4*, 299-309. 10.1038/nrn1078.

44. Laplante, M., and Sabatini, David M. (2012). mTOR Signaling in Growth Control and Disease. Cell *149*, 274-293. 10.1016/j.cell.2012.03.017.

45. Chen, G., Chen, S.M., Wang, X., Ding, X.F., Ding, J., and Meng, L.H. (2012). Inhibition of chemokine (CXC motif) ligand 12/chemokine (CXC motif) receptor 4 axis (CXCL12/CXCR4)-mediated cell migration by targeting mammalian target of rapamycin (mTOR) pathway in human gastric carcinoma cells. J Biol Chem *287*, 12132-12141. 10.1074/jbc.M111.302299.

46. Vogeser, M., König, D., Frey, I., Predel, H.-G., Parhofer, K.G., and Berg, A. (2007). Fasting serum insulin and the homeostasis model of insulin resistance (HOMA-IR) in the monitoring of lifestyle interventions in obese persons. Clinical Biochemistry *40*, 964-968. https://doi.org/10.1016/j.clinbiochem.2007.05.009.

47. Shimizu, Y., Kondo, K., Hayashida, R., Sasaki, K.I., Ohtsuka, M., Fukumoto, Y., Takashima, S., Inoue, O., Usui, S., Takamura, M., et al. (2022). Therapeutic angiogenesis for patients with no-option critical limb ischemia by adipose-derived regenerative cells: TACT-ADRC multicenter trial. Angiogenesis. 10.1007/s10456-022-09844-7.

48. Gerhard-Herman, M.D., Gornik, H.L., Barrett, C., Barshes, N.R., Corriere, M.A., Drachman, D.E., Fleisher, L.A., Fowkes, F.G.R., Hamburg, N.M., Kinlay, S., et al. (2017). 2016 AHA/ACC Guideline on the Management of Patients With Lower Extremity Peripheral Artery Disease: Executive Summary: A Report of the American College of Cardiology/American Heart Association Task Force on Clinical Practice Guidelines. Circulation *135*, e686-e725. doi:10.1161/CIR.0000000000000470.

49. Bode, D., Cull, A.H., Rubio-Lara, J.A., and Kent, D.G. (2021). Exploiting Single-Cell Tools in Gene and Cell Therapy. Frontiers in Immunology *12*. 10.3389/fimmu.2021.702636.

50. Hashmi, S., Ahmed, M., Murad, M.H., Litzow, M.R., Adams, R.H., Ball, L.M., Prasad, V.K., Kebriaei, P., and Ringden, O. (2016). Survival after mesenchymal stromal cell therapy in steroid-refractory acute graft-versus-host disease: systematic review and meta-analysis. The Lancet Haematology *3*, e45-e52. https://doi.org/10.1016/S2352-3026(15)00224-0.

51. Kelly, K., and Rasko, J.E.J. (2021). Mesenchymal Stromal Cells for the Treatment of Graft Versus Host Disease. Frontiers in Immunology *12*. 10.3389/fimmu.2021.761616.

52. Smith, R.J.P., Faroni, A., Barrow, J.R., Soul, J., and Reid, A.J. (2021). The angiogenic potential of CD271+ human adipose tissue-derived mesenchymal stem cells. Stem Cell Research & Therapy *12*, 160. 10.1186/s13287-021-02177-0.

53. Kohli, N., Al-Delfi, I.R.T., Snow, M., Sakamoto, T., Miyazaki, T., Nakajima, H., Uchida, K., and Johnson, W.E.B. (2019). CD271-selected mesenchymal stem cells from adipose tissue enhance cartilage repair and are less angiogenic than plastic adherent mesenchymal stem cells. Scientific Reports *9*, 3194. 10.1038/s41598-019-39715-z.

54. Méndez-Maldonado, K., Vega-López, G.A., Aybar, M.J., and Velasco, I. (2020). Neurogenesis From Neural Crest Cells: Molecular Mechanisms in the Formation of Cranial Nerves and Ganglia. Frontiers in Cell and Developmental Biology *8*. 10.3389/fcell.2020.00635.

55. Xie, Y., Jin, Y., Merenick, B.L., Ding, M., Fetalvero, K.M., Wagner, R.J., Mai, A., Gleim, S., Tucker, D.F., Birnbaum, M.J., et al. (2015). Phosphorylation of GATA-6 is required for vascular smooth muscle cell differentiation after mTORC1 inhibition. Science Signaling *8*, ra44-ra44. doi:10.1126/scisignal.2005482.

56. Ormazabal, V., Nair, S., Elfeky, O., Aguayo, C., Salomon, C., and Zuñiga, F.A. (2018). Association between insulin resistance and the development of cardiovascular disease. Cardiovasc Diabetol *17*, 122. 10.1186/s12933-018-0762-4.

57. Um, S.H., Frigerio, F., Watanabe, M., Picard, F., Joaquin, M., Sticker, M., Fumagalli, S., Allegrini, P.R., Kozma, S.C., Auwerx, J., and Thomas, G. (2004). Absence of S6K1 protects against age- and diet-induced obesity while enhancing insulin sensitivity. Nature *431*, 200-205. 10.1038/nature02866.

58. Rupnick, M.A., Panigrahy, D., Zhang, C.Y., Dallabrida, S.M., Lowell, B.B., Langer, R., and Folkman, M.J. (2002). Adipose tissue mass can be regulated through the vasculature. Proceedings of the National Academy of Sciences *99*, 10730-10735. 10.1073/pnas.162349799.

59. Xu, H., Barnes, G.T., Yang, Q., Tan, G., Yang, D., Chou, C.J., Sole, J., Nichols, A., Ross, J.S., Tartaglia, L.a., and Others (2003). Chronic inflammation in fat plays a crucial role in the development of obesity-related insulin resistance. Journal of Clinical Investigation *112*, 1821-1830. 10.1172/JCI200319451.Introduction.

60. Goossens, G.H., Bizzarri, A., Venteclef, N., Essers, Y., Cleutjens, J.P., Konings, E., Jocken, J.W.E., Čajlaković, M., Ribitsch, V., Clément, K., and Blaak, E.E. (2011). Increased adipose tissue oxygen tension in obese compared with lean men is accompanied by insulin resistance, impaired adipose tissue capillarization, and inflammation. Circulation *124*, 67-76. 10.1161/CIRCULATIONAHA.111.027813.

61. Crewe, C., An, Y.A., and Scherer, P.E. (2017). The ominous triad of adipose tissue dysfunction: Inflammation, fibrosis, and impaired angiogenesis. Journal of Clinical Investigation *127*, 74-82. 10.1172/JCI88883.

62. Gimble, J.M., Bunnell, B.A., Chiu, E.S., and Guilak, F. (2011). Concise Review: Adipose-Derived Stromal Vascular Fraction Cells and Stem Cells: Let's Not Get Lost in Translation. Stem Cells *29*, 749-754. 10.1002/stem.629.

63. Varghese, J., Griffin, M., Mosahebi, A., and Butler, P. (2017). Systematic review of patient factors affecting adipose stem cell viability and function: implications for regenerative therapy. Stem Cell Research & Therapy *8*, 45-45. 10.1186/s13287-017-0483-8.

64. Rennert, R.C., Sorkin, M., Januszyk, M., Duscher, D., Kosaraju, R., Chung, M.T., Lennon, J., Radiya-Dixit, A., Raghvendra, S., Maan, Z.N., et al. (2014). Diabetes impairs the angiogenic potential of adipose-derived stem cells by selectively depleting cellular subpopulations. Stem Cell Research & Therapy *5*, 1-12. 10.1186/scrt468.

65. Inoue, O., Usui, S., Takashima, S.I., Nomura, A., Yamaguchi, K., Takeda, Y., Goten, C., Hamaoka, T., Ootsuji, H., Murai, H., et al. (2019). Diabetes impairs the angiogenic capacity of human adipose-derived stem cells by reducing the CD271(+) subpopulation in adipose tissue. Biochem Biophys Res Commun *517*, 369-375. 10.1016/j.bbrc.2019.07.081.

66. Stoeckius, M., Hafemeister, C., Stephenson, W., Houck-Loomis, B., Chattopadhyay, P.K., Swerdlow, H., Satija, R., and Smibert, P. (2017). Simultaneous epitope and transcriptome measurement in single cells. Nature Methods *14*, 865-868. 10.1038/nmeth.4380.

67. Katagiri, T., Kondo, K., Shibata, R., Hayashida, R., Shintani, S., Yamaguchi, S., Shimizu, Y., Unno, K., Kikuchi, R., Kodama, A., et al. (2020). Therapeutic angiogenesis using autologous adipose-derived regenerative cells in patients with critical limb ischaemia in Japan: a clinical pilot study. Scientific Reports *10*, 1-12. 10.1038/s41598-020-73096-y.

68. Vijay, J., Gauthier, M.F., Biswell, R.L., Louiselle, D.A., Johnston, J.J., Cheung, W.A., Belden, B.,

Pramatarova, A., Biertho, L., Gibson, M., et al. (2020). Single-cell analysis of human adipose tissue identifies depot and disease specific cell types. Nat Metab *2*, 97-109. 10.1038/s42255-019-0152-6.

69. Rondini, E.A., Ramseyer, V.D., Burl, R.B., Pique-Regi, R., and Granneman, J.G. (2021). Single cell functional genomics reveals plasticity of subcutaneous white adipose tissue (WAT) during early postnatal development. Mol Metab *53*, 101307. 10.1016/j.molmet.2021.101307.

70. Ganan-Gomez, I., Yang, H., Ma, F., Montalban-Bravo, G., Thongon, N., Marchica, V., Richard-Carpentier, G., Chien, K., Manyam, G., Wang, F., et al. (2022). Stem cell architecture drives myelodysplastic syndrome progression and predicts response to venetoclax-based therapy. Nat Med *28*, 557-567. 10.1038/s41591-022-01696-4.

71. Moison, C., Spinella, J.-F., Chagraoui, J., Lavallée, V.-P., Lehnertz, B., Thiollier, C., Boivin, I., Mayotte, N., MacRae, T., Marinier, A., et al. (2022). HMGA2 expression defines a subset of human AML with immature transcriptional signature and vulnerability to G2/M inhibition. Blood Advances *6*, 4793-4806. https://doi.org/10.1182/bloodadvances.2021005828.

72. Korsunsky, I., Millard, N., Fan, J., Slowikowski, K., Zhang, F., Wei, K., Baglaenko, Y., Brenner, M., Loh, P.r., and Raychaudhuri, S. (2019). Fast, sensitive and accurate integration of single-cell data with Harmony. Nature Methods *16*, 1289-1296. 10.1038/s41592-019-0619-0.

73. Vuong, H., Truong, T., Phan, T., and Pham, S. (2020). Venice: A New Algorithm for Finding Marker Genes in Single-Cell Transcriptomic Data. bioRxiv, 2020.2011.2016.384479. 10.1101/2020.11.16.384479.

74. Consortium, G.O. (2004). The Gene Ontology (GO) database and informatics resource. Nucleic Acids Research *32*, D258-D261. 10.1093/nar/gkh036.

75. Le, T., Phan, T., Pham, M., Tran, D., Lam, L., Nguyen, T., Truong, T., Vuong, H., Luu, T., Phung, N., et al. (2020). BBrowser: Making single-cell data easily accessible. bioRxiv, 2020.2012.2011.414136-412020.414112.414111.414136. 10.1101/2020.12.11.414136.